Accepted Manuscript

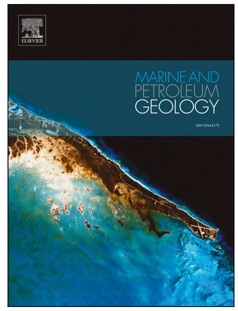

Towards process-based geological reservoir modelling: obtaining basin-scale constraints from seismic and well data

Quinto Sacchi , Gert Jan Weltje , Francesca Verga

PII: S0264-8172(14)00364-X

DOI: 10.1016/j.marpetgeo.2014.11.002

Reference: JMPG 2092

To appear in: *Marine and Petroleum Geology*

Received Date: 20 December 2013

Revised Date: 24 October 2014

Accepted Date: 20 November 2014

Please cite this article as: Sacchi, Q., Weltje, G.J., Verga, F., Towards process-based geological reservoir modelling: obtaining basin-scale constraints from seismic and well data, *Marine and Petroleum Geology* (2014), doi: 10.1016/j.marpetgeo.2014.11.002.

TOWARDS PROCESS-BASED GEOLOGICAL RESERVOIR MODELLING: OBTAINING BASIN-SCALE CONSTRAINTS FROM SEISMIC AND WELL DATA

Quinto Sacchi[1], Gert Jan Weltje[2,3], Francesca Verga[1,*]

[1] Politecnico di Torino, Engineering Faculty, Department of Environment, Land and Infrastructure Engineering, Corso Duca degli Abruzzi 24, 10129, Torino, Italy.
[2] Delft University of Technology, Department of Geoscience and Engineering, Stevinweg 1, NL-2628CN, Delft, The Netherlands.
[3] Present address: University of Leuven, Department of Earth and Environmental Sciences, Geology Division, Celestijnenlaan 200E, 3001 Leuven-Heverlee, Belgium.

Keywords: process-based stratigraphic simulation; model inversion; uncertainty; inference approach; sub-grid parameterization

Highlights:

- Fluvio-deltaic stratigraphy was simulated with a 2DH process-based model
- Goodness of fit functions were used to infer boundary conditions from subsurface data
- Information content of seismic and well data was evaluated
- Depth of reservoir top across basin is best predictor of reservoir lithology

* **Corresponding author**: Corso Duca degli Abruzzi 24, 10129, Torino, Italy; e-mail: verga.francesca@polito.it; phone: +390110907644; fax: +390110907699;

ABSTRACT

Forward stratigraphic modelling aims at representing the spatial distribution of lithology as a function of physical processes and environmental conditions at the time of deposition so as to integrate geological knowledge into the reservoir modelling workflow, thus increasing predictive capabilities of reservoir models and efficient exploitation of hydrocarbons. Application of process-based models in inverse mode is not yet well-established due to our limited insight into the information content of common subsurface data and the computational overhead involved.

In this paper we examine inverse modelling of stratigraphy by using a typical dataset acquired in the hydrocarbon industry, which consists of seismic data and standard logs from a limited number of wells. The approach is based on the use of a forward model called SimClast, developed at Delft University of Technology, to generate facies distribution and architecture at the regional scale. Three different goodness of fit functions were proposed for model inversion, following an inference approach. A synthetic reservoir unit was used to investigate the impact of the uncertainty affecting the input parameters and the information content of seismic and well data.

The case study showed that the model was more sensitive to the initial topography and to the location of the sediment entry point than to sea level. The depth of the seismic reflector corresponding to the top-reservoir surface was the most informative data source; the initial and boundary conditions of the simulation were constrained by evaluating the depth of this reflector across the whole basin area. In the reservoir area, where the seismic-to-well tie was established, the depth of the reservoir top does not give enough information for constraining the model parameters. Our results thus indicate that evaluation of basin-scale data permits reduction of uncertainty in (geostatistical) reservoir models relative to the current workflow, in which only local data are used. Effective use of well data to generate reservoir models conditioned to basin-scale scenarios requires post-processing methods to downscale the output of the forward model used in the experiments.

1 INTRODUCTION

The current workflow for obtaining static reservoir models relies on integration of quantitative well and seismic data by geostatistical (geometric-stochastic) methods. Kriging-like procedures are used to build a “best-guess” static reservoir model, from which an ensemble of equiprobable realisations is produced by conditional simulation (Deutsch, 2002). Conditional simulation implies that the large-scale geometry of a reservoir (and its enveloping geological unit) as derived from seismics is respected and well data are honoured. Each realisation is transformed into a continuous 3-D porosity and permeability field by appropriate averaging (upscaling) procedures to serve as boundary conditions for dynamic models of reservoir behaviour. Uncertainties associated with reservoir behaviour are modelled by regarding the ensemble of equiprobable realisations obtained by conditional simulation as a representative sample of a population of (geologically realistic) subsurface models that is consistent with the observations. The underlying geological scenario is in most cases the main source of uncertainty (Deutsch, 2002; Bentley and Smith, 2008) and therefore multiple scenarios should be subjected to this geostatistical modelling workflow for any reservoir.

In the geostatistical approach to geological reservoir modelling, the aim is to mimic the present-day spatial distribution of geological entities without taking into account how a particular spatial distribution of lithology (porosity and permeability) has been generated. Geological objects, such as channel belts, shale lenses, and sandy lobes are introduced into such models by invoking templates, so called "analogues" taken from outcrops of rocks inferred to have formed under similar conditions (Deutsch, 2002). This “product-based” approach to prediction of reservoir architecture does provides limited opportunities for incorporating knowledge of the physical laws which govern basin filling into the modelling workflow (Karssenberg et al., 2001; Imhof and Sharma, 2006; Charvin et al., 2009, 2011; Weltje et al., 2013). A recently conducted experiment in which a continuous outcrop was sparsely sampled to mimic subsurface data (Deveugle et al., 2014) illustrates the limitations of state-of-the-art geostatistical algorithms for prediction of lithology between wells.

The use of process-based stratigraphic simulation models facilitates the integration of basin-scale geological constraints into static reservoir models by providing quantitative predictions of the spatial distribution of lithology (stratigraphic architecture) based on geological information that is in principle independent of the local data to which reservoir models are typically conditioned.

The capability to predict stratigraphic architecture is relevant to reservoir modelling because high-resolution sequence-stratigraphic representations of (local) basin-fill architecture may be used to guide different stages of the reservoir-modelling workflow: from the early phase of stratal pattern reconstruction by well correlation and definition of possible depositional scenarios (Wendebourg and Harbaugh, 1997; Burgess et al., 2006; Falivene et al., 2014) to the final stage of constraining stochastic lithofacies distributions for the assessment of reservoir volumes and connectivity, and the planning of infill wells (Doligez et al., 1999). Instead of building inferences about reservoir architecture solely upon models which honour the well data of a particular reservoir, which may not contain enough information to constrain stochastic models (Karssenberg et al., 2001), process-based stratigraphic modelling allows us to reduce the solution space of reservoir architecture to a subset of models which also honour basin-scale geological constraints. For practical purposes, however, the added value of stratigraphic modelling relies on our capability to condition these highly non-linear models to case-specific observations, such as seismic and well data (Burton et al., 1987; Heller et al., 1993; Lessenger and Cross, 1996; Cross and Lessenger, 1999; Bornholdt et al., 1999; Wijns et al., 2004; Imhof and Sharma, 2006; Falivene et al., 2014). If this can be accomplished, we may narrow down the range of possible scenarios (realisations) in the exploration stage, which should result in more reliable uncertainty estimates associated with reservoir-architecture models.

In this study we focus on the first step of the workflow, i.e. conditioning of a process-based model to seismic and well data. We carry out stratigraphic simulations with SimClast, an aggregated basin-scale process-based model of a fluvio-deltaic system with sub-grid parameterizations of fluvial channel networks and coastal dynamics (Dalman and Weltje, 2008, 2012). SimClast is a so-called 2DH model (depth-averaged model of flow in the two-dimensional horizontal plane). The term sub-grid parameterization originated in the field of computational fluid dynamics (Meneveau, 2010). In the case of SimClast, it refers to the implementation of processes which govern the evolution of drainage networks (such as avulsions) as sub-grid scale routines into the large-scale basin-filling model. The visualization and investigation of the sub-grid alluvial stratigraphy generated implicitly by the model may be performed by post-processing of model output in order to attain the level of detail required for geological reservoir modeling.

It is well known that the parameters of a model can be inferred by means of inverse methods (optimization or sample based). Inversion of highly non-linear models of sedimentary systems is an iterative process in which the stratigraphic model is run, the output is compared with the data according to an objective function (or likelihood function in Bayesian approaches), the parameters are adjusted by means of the selected technique and the model is run again until a satisfactory match with the target has been reached (Lerche, 1992, 1996; Bornholdt et al. 1999; Wijns et al., 2004; Charvin et al., 2009, Karssenberg et al., 2001; Karssenberg et al., 2007; Verga et al., 2013). One of the potential problems in stratigraphic inversion is the non-uniqueness of the solution, i.e. multiple solutions which fit the data equally (or nearly) as well, even in cases where a good match between model and data has been achieved. Moreover, the inversion of sedimentary models tends to be computationally expensive and is sometimes regarded as unfeasible (Wijns et al., 2004; Burgess, 2012). An alternative method, suited for situations in which limited data are available (Heller et al., 1993; Burgess et al., 2006) consists of systematically searching the likely parameter space in order to form a map of the model properties (e.g. spatial distribution of net to gross). In the approach adopted in this study, each input parameter was assumed to follow a uniform distribution over a given interval. The solution space was explored with a Quasi-Monte Carlo method in order to obtain a set of solutions corresponding to each possible combination of input parameters. Conditioning of the model to well and seismic data was achieved by an inferential approach, using different goodness of fit functions, i.e. functions expressing the misfit between simulated data and a reference case mimicking real data. Because the solution space contained a ‘reference case’, the effectiveness of the goodness of fit functions could be evaluated in the light of possible limitations of the forward model and/or the data. This approach allowed exploration of the parameter space and robust assessment of the uncertainty in a fully non-linear manner. This approach differs from local (i.e. gradient methods) and global (i.e. Genetic Algorithm) optimization methods, which are primarily designed to find a single ‘best-fit’ solution (Lerche, 1996), in that it was aimed at identifying multiple scenarios of input parameters characterized by a likely stratigraphic realization. Systematic exploration of the parameter space provided the analysis of the influence of each of the parameters, and allows us to evaluate how the uncertainty of input parameters propagated to the modelled stratigraphy.

In a follow-up study of the present paper we intend to use the obtained basin-scale results to constrain sedimentary architecture at the reservoir scale. This will allow us to assess how the associated uncertainty propagates to the reservoir scale, opening the way to a full-risk analysis on the hydrocarbons initially in place and the recoverable reserves as a function of a given field development plan.

1.1 Process-based stratigraphic simulators

Stratigraphic forward models may be subdivided into two main categories: geometric and dynamic models (Paola, 2000; Burgess, 2012). Geometric models are relatively simple as they do not aim at describing the physical processes involved, but instead focus on direct simulation of the resulting stratal geometries (Burton et al., 1987; Bowman and Vail, 1999; Cross and Lessenger, 1999). Dynamic models are more complex as they attempt to simulate time-dependent erosion and sedimentation processes using empirical and/or process-based equations. Two main approaches can be distinguished within the latter method: hydraulic models and diffusion-based models. Hydraulic models use flow laws based on simplifications of the Navier-Stokes equations to describe sediment transport and deposition (Tetzlaff and Harbaugh, 1989; Griffiths et al., 2001; Warner et al., 2008), whereas diffusion-based models represent sediment transport and deposition as a function of the topographic gradient (Granjeon and Joseph, 1999; Meijer, 2002). Stratigraphic forward models may also be classified in terms of targeted sedimentary environments. Siliciclastic models describe the evolving forms of clastic basin fills as a function of physical erosion, transport and deposition (Tetzlaff and Harbaugh, 1989; Storms et al., 2002; Clevis et al., 2003; Dalman and Weltje, 2012), whereas carbonate models implement bio-chemical constraints to calculate *in-situ* precipitation and production of carbonate sediment (Burgess, 2001, Warrlich et al., 2008). Models of complete sedimentary systems are obtained by dynamically coupling single-environment models (Hutton and Syvitski, 2008; Warner et al., 2008).

The synthetic reservoir studied in this paper consists of sediments deposited in a fluvio-deltaic environment. The forward model employed is SimClast (Dalman and Weltje, 2008, 2012), an aggregated, basin-scale 2DH stratigraphic model which comprises several coupled sedimentary environments. It was developed between 2005 and 2009 at Delft University of Technology to study the complex interactions between fluvial and marine processes and their effects on fluvio-deltaic stratigraphy. The numerical model uses loading and accounting schemes based on Meijer (2002). The model is capable of simulating fluvial channel network dynamics, plume deposition and wave-induced cross-shore and long-shore transport. Smallscale processes governing the dynamics of fluvial channel networks and shoreface evolution have been implemented as sub-grid parameterizations, with the intent to achieve realistic morphodynamic behaviour and stratigraphic architecture without significantly compromising computational efficiency. Sub-grid sediment transport and channelization are derived from physical equations, capable of producing convergent and divergent drainage networks, trunk channels and, most importantly, a detailed representation of crevasses, avulsions and bifurcations (Dalman and Weltje, 2008).

SimClast can model siliciclastic sedimentary basins up to 10^6 km^2 (with spatial resolution of 1 to 5 km) over time scales from 10^3 to 10^6 years (with temporal resolution of 1 to 10 years). Model output consists of multiple maps (snapshots) of topography, sedimentation pattern and liquid discharge. Furthermore, a volume comprising discrete stratigraphic information on sediment thickness, grain size and age (spatially averaged over each cell) is created for the entire grid. Additional information on channel architecture may be extracted from the sub-grid parameterization. The channel-belt pattern is described in terms of fluvial style (braided or meandering), the volume of channelized deposits, the flow direction and channel-top elevation for each grid cell. Exact locations, widths and thicknesses of the channel-belt deposits are not resolved, but can be constructed by dedicated post-processing software employing geostatistical simulation techniques. The sub-grid parameterization is the main reason for the high computational efficiency of SimClast compared to other process-based models which provide this level of architectural detail during runtime.

1.2 Reference case and synthetic dataset

In order to perform simulations with SimClast several environmental parameters need to be set: the initial surface and subsurface sediment properties, (spatially variable) subsidence, sea level, river inflow location(s), liquid discharge and sediment supply, grain size of the sediment feed, wave regime, and the current pattern at the grid boundaries. The reference case consists of a synthetic dataset generated by SimClast. We selected a reservoir unit corresponding to one major aggradational episode within a fluvio-deltaic sedimentary system, which took 8000 simulated years to form. Over the course of this comparatively short time interval (geologically speaking), the sediment entry point did not migrate laterally, sea level was stable, and climate fluctuations as mirrored in changes of liquid and solid discharge were absent. We opted for the maximum spatial and temporal resolution and used grid cells of 1x1 km and time steps of 1 year. The grid extended 50 km in the East-West direction and 47 km in the North-South direction. As each simulation encompassed only 8000 years, the simulation time was short enough for systematic searches of the parameter space.

The objective of the simulations was to illustrate the effect of three main environmental parameters on reservoir properties:

- Initial topography;
- Location of water/sediment entry point;
- Sea level.

The three parameters taken into consideration are by far the most important forcing factors, in view of the short time span involved in the generation of the reservoir unit under consideration. Hence, each model run was conducted under time-invariant forcing factors, i.e. constant sea level, liquid discharge and sediment supply. The grain size of the sediment feed comprised two discrete classes: sand, representing the reservoir units (such as crevasse splays, channel deposits, and levees), and clay, representing the floodplain deposits. A base case was generated by assigning an initial topographic elevation ranging from 24 m to 74 m above the reference level, with an average slope of about 0.1% dipping to the north-east. The sediment entry point was fixed at the intermediate location (grid cell number 24, corresponding to 30 km) along the western edge of the model and the sea level was set equal to 44.5 m above the topographic reference level. It was assumed that four wells (labeled A, B, C and D) had been drilled to explore and delimit the reservoir. Figure 1 shows the vertically averaged net-to-gross ratio (the proportion of sand), the reservoir area and the positions of the four wells in the central part of the model. A synthetic dataset was generated from the reference case with the objective to mimic the typical data available for geological reservoir modelling in the appraisal phase of a field's life cycle. The dataset consisted of:

- The lithology intercepted by the wells (fig. 2), which is usually derived from the analysis of the cuttings during perforation as well as from the correlation between wireline logs (such as gamma-ray or spontaneous potential logs) and core data. Downscaling the SimClast output to the reservoir scale was achieved by post-processing the sub-grid information to obtain a 3D distribution of the channel volume fraction, representative of the channel occurrence probability (P_{CH}) for each grid cell. The lithology has a vertical resolution of 10 cm, which reflects the quality of the underlying data (core descriptions, FMI logs, or deconvolved 'conventional' well logs). The data are schematically interpreted as channel-belt deposits (thick sands), crevasse splays (thin sands), and floodplain fines.

- The top reservoir surface extracted from the basin scale simulation. This information is typically defined through seismic interpretation and is subject to uncertainty due to the adoption of a velocity model for time-to-depth conversion.
- The well control points for bottom (initial topography) and top surfaces, which are typically defined from well log analysis and, as a consequence, constitute the least uncertain data.

2 INPUT DISTRIBUTIONS OF UNKNOWN PARAMETERS

This study focused on the initial topography, the sea level and the sediment entry point. Since the exact value of the parameters characterizing the forward model cannot be estimated *a priori*, a considerable range of uncertainty was assumed for each parameter.

2.1 Initial topography

The geometry of the stratigraphic surfaces bounding a reservoir is inferred from seismic data. The seismic data are then integrated with well data to define a velocity model for time-to-depth conversion. Usually, the availability of 3D seismic data is limited to the reservoir zone and its immediate surroundings. The 2D seismic data acquired in the exploration phase has a regional coverage, and their density typically allows identification of large-scale geological structures through interpolation. The difference in the level of knowledge of the reservoir zone compared to the surrounding region is further emphasized by the well-to-seismic ties which drastically reduce the uncertainty associated with time-to-depth conversion.

For the purpose of this study we assumed that no wells were available to constrain the seismic and stratigraphy at the regional scale except for the four wells which had intercepted the reservoir zone, located in the central area of the model grid. The implication of this assumption was a significant uncertainty of the initial topography away from the reservoir zone. The uncertainty associated with the initial topography was captured by a set of 22 realizations (fig. 3), which were generated by introducing the following perturbation to generate the surface realizations S_r:

$$S_r = S_{bc} + U_{1\sigma} U_{sgs} \qquad (1)$$

where:

S_{bc}: base case, or reference surface

$U_{1\sigma}$: depth error on the reference surface with assigned standard deviation σ

U_{sgs}: stochastic error surface obtained by Sequential Gaussian simulation with zero mean and unit standard deviation, conditioned to wells A, B, C, and D.

All realizations were based on the semi-variogram model derived from the reference surface, and were tied to the well locations (A, B, C, D). The goodness of fit of the realizations is represented by their similarity to the reference surface. The misfit was evaluated taking into account the uncertainty of the velocity model used to convert the seismic data from time to depth. Misfits up to 5 m were considered negligible, in agreement with assumed uncertainties of seismic-to-well ties. The misfit was computed over the entire basin area and over the reservoir zone only (fig. 4). As a consequence of constraining all the realizations to well data, the uncertainty decreases towards the well locations. Therefore, all initial topographies are less uncertain in the reservoir area than in the surrounding area. The realizations were ranked according to their goodness of fit over the entire basin area: no. 1 (representing the actual initial topography) corresponds to the best-fit topography and no. 22 to the worst fitting realisation.

2.2 Sediment entry point

Soft constraints on the sediment entry point are commonly provided by the knowledge of regional paleo-topographic gradients and lateral thickness and/or grain-size trends. In the present study, a single sediment entry point was considered at the western edge of the model grid, broadly consistent with the general dipping of the initial topography towards the northeast. A range of uncertainty of 20 km in the North-South direction was assumed (grid cell numbers 15 to 34, corresponding to the range 20-40 km), as shown in figure 5.

2.3 Sea level

The sea level may be constrained by paleo-bathymetric analysis or by facies analysis at the well locations. We assumed that the sea level was constant during the geologically short simulated period (8000 years). A range of variability of 35 meters around the reference value, thus a variation between 30.5 and 65.5 m, was considered (fig. 5).

3 MODEL INVERSION AND UNCERTAINTY EVALUATION

In order to assess the uncertainty of the input parameters, we propagated the probability distribution functions (PDFs) of the input distributions through the model to obtain the PDF of the output distributions.

Methods to determine the probability distribution of an output quantity from the probability distributions assigned to the input quantities may be analytical (Taylor, 1982; Amaefule and Keelan, 1989), numerical (Bornholdt et al. 1999; Nakayama, 2000; Charvin et al., 2009; JCGM, 2008; Viberti et al., 2012) or interactive (Boschetti and Moresi, 2001, Wijns et al, 2004). Analytical methods of error propagation, although preferable because they are exact, were discarded because they are applicable to simple cases only (i.e. linear or linearized problems). Instead, a Quasi-Monte Carlo approach with systematic sampling was chosen. In this method, the input distribution is approximated by sampling according to a specific pattern, for example at equally-spaced intervals along a line or a grid. The first element is selected randomly and the selection of the remaining elements is determined by the pattern (Cochran, 1963). This kind of sampling is also called quasi-random (Naval, 2009). It differs from a classical Monte Carlo because a quasi-random sequence in place of a random sequence is exploited in the sampling stage (Caflisch, 1998). A Quasi-Monte Carlo method requires a smaller number of samples to get the same accuracy as a Monte Carlo method when the population is homogeneous because it emphasizes full coverage of the area of interest (Pal, 1998) and eliminates the clumping phenomenon, which is a limiting factor in the accuracy of the Monte Carlo method (Caflisch, 1998). As a consequence, the computational cost is significantly reduced.

The input parameters of the stratigraphic simulation were assumed to be independent and uniformly distributed. Theoretically a dependence between sediment entry point, sea level and initial topography is present but it had already been taken into account in the preliminary study conducted to choose the range of variation of each parameter. Within the chosen ranges the degree of uncertainty over each single parameter makes the independence assumption reasonable. In this study, the forward stratigraphic model was applied to each sample of input parameters, giving a set of results that constituted the output distribution. Initially, scenarios representative of the uncertainty affecting the input parameters were selected by systematic sampling in a reasonable range, defined from *a priori* knowledge of the system. The sampling pattern was based on considerations arising from preliminary sensitivity analyses. Initially, a coarse grid based on equally-spaced sampling was defined for all parameters, resulting in the definition of 1100 scenarios. In a second phase, a locally refined parameter space analysis was conducted around the most promising parameter sets identified in the first phase. Sampling was then conducted with a quasi-uniform distribution on the new parameter space. Approximately 2000 scenarios were realized overall. Sensitivity analysis showed that a further refinement would not add any valuable information. .

The input parameters were considered variables described by a probability distribution. This probability distribution (first stage distribution) was formulated before the simulation results were compared with the available data. However, the uncertainty affecting the input parameters was significantly reduced by excluding all the scenarios that did not fit the available data. When a sample (i.e. a parameter set composed by initial topography, sea level and sediment entry point) was taken, the outcome (i.e. the corresponding basin simulation results) was observed and compared with the available data (posterior knowledge). The goodness of fit between the simulated and reference data was expressed as the probability that the available data could be reproduced by a model characterized by the sampled set of input parameters. A misfit threshold was then introduced in order to discard basin scenarios that had high misfits and, in turn, to reduce the uncertainty associated with the input parameters (second stage distribution).

The entire approach was conceived so as to be applicable to real-world cases where the typical dataset consists of well and seismic data. Thus, we compared the stratigraphic surfaces provided by basin modeling with the stratigraphic surfaces obtained from seismic interpretation, and compared the lithology predicted by the model with the lithology observed at the well locations. In the case analyzed in this study (fig. 1) the lithology was assumed to be available at the sites of four appraisal wells A, B, C and D (fig. 2).

Caution is needed when comparing basin-scale simulation results with available hard data, such as well lithology. In fact, well logs provide information on the system architecture at the reservoir scale, whereas the basin-scale simulations provide the spatial distribution of entire channel belts, which is one order of magnitude larger. Although the channel-belt volume, the number of channels, the direction of the channel belt and the depth of the channels bottom are implicitly given by the basin model, these quantities cannot be directly converted into a prediction of the well lithology without post-processing of the model output because lithology is not spatially uniform within each grid cell. Therefore, the comparison was limited to the elevation of the reservoir tops at the wells and to the probability that a channel was intercepted by a well. Finally, a goodness of fit function was calculated to account for the mismatch with soft data, expressing how the simulated top surface fits the seismic top surface. The uncertainty associated with the top reservoir surface derived from seismic data is mainly due to the velocity model used to convert two-way travel time into depth. This uncertainty was considered by introducing a confidence interval for the top surface. The mathematical definitions of the goodness of fit functions are reported in the Appendix.

4 RESULTS

In order to analyze the propagation of uncertainty associated with the selected input parameters (sediment entry point, sea level and initial topography) to the model output, we examined the variability of several quantities extracted from the realizations.

The predicted volume fraction of the channelized deposits in the reservoir area is shown as a function of the input parameters in figure 6. This quantity is influenced by the location of the sediment entry point (giving maxima for the northernmost locations) and to a lesser extent by the initial topography. The corresponding histogram shows that predictions of the volume fraction of the channelized deposits range between 20% and 40% (fig. 7a); this interval contains the value of the reference case (35%). The distribution of the channel-belt directions in the reservoir area (fig. 7b) is not sensitive to the input parameters. In fact, it is symmetrical, with a mean of 270° and variance of 45° (the value of the reference case is 270°).

The degree of similarity in terms of stratigraphic architecture and channel-occurrence probability among simulated scenarios was examined with a hierarchical cluster analysis technique. The inter-cluster distance was calculated using the squared Euclidean metric. Several linkage approaches were considered (Hastie et al. 2009), but the inner squared distance (Ward, 1963), i.e. the minimization of the total within-cluster variance, proved to give the best separation between clusters.

Four clusters were identified based on the elevation of the bounding surfaces in the overall basin area. The cutoff distance, distinguishing between clusters, was chosen in order to maximize the distances among the clusters, based on the dendrogram plot (fig. 8a). In the dendrogram it is clearly visible that the objects tend to form four different groups. These groups are connected by three longer links, which are inconsistent with the links below them in the hierarchy. The location of the sediment entry point and the initial topography appear to be the dominant controlling factors on the shape of the reflectors bounding the reservoir unit (fig. 8b). A sharp discontinuity in the cluster affiliation occurs in the proximity of the central position of the sediment entry point (i.e. 30 km), which corresponds to the actual location. Similar results were obtained by clustering the scenarios based on the channel occurrence probability in the reservoir area. Three main clusters were identified in this case (fig. 9a). Again, clusters appear to be controlled by the location of the sediment entry point and by the initial topography (fig. 9b). All scenarios in which the sediment entry points are located in the northern area (from 35 km to 40 km) belong to the same cluster.

The values of the goodness of fit function used to evaluate the mismatch of the stratigraphic surfaces with the available seismic data (Eq. 6) are shown in figures 10 and 11. The goodness of fit of the stratigraphic surface showed a strong dependence on the location of the sediment entry point and on the initial topography, and much less on sea-level variations (fig. 10). A roughly symmetrical impact of the sediment entry point relative to the reference case (i.e. 30 km) can be observed. The 100 most likely scenarios out of the 2000 basin simulations (fig. 10b) indicate that the sediment entry point was located between 26 and 32 km and that the sea level varied between 41.5 m and 49.5 m. Furthermore, only a few likely initial topographies were identified. If the goodness of fit evaluation of the top surface is limited to the reservoir area (fig. 11), trends related to the initial topography cannot be observed. The difference between basin and reservoir-area goodness of fit inferred from seismic data is evident from the histograms displayed in Figure 12, where the scenarios showing a negligible discrepancy with the reference case represent 17% of the simulations when evaluated on the reservoir area only (fig. 12a) against 4% of the simulations when the whole basin area is taken into account (fig. 12b). This is a direct consequence of constraining all the initial topographies to the well data. Therefore, the modelled top surfaces were subject to less uncertainty in the reservoir area than in the surrounding area and did not contain much information on stratigraphic variability.

The goodness of fit relative to the well data was based on the well tops (representing the depth at which each well intersected the top reservoir surface) and on the lithology of each well (a sand/shale sequence representing channel-belt versus floodplain deposits). Figure 13 shows the depth mismatch between the well tops for wells A, B, C, D and the top surfaces at the corresponding grid cells (Eq. 2). It can be observed that most scenarios are characterized by a low misfit. The general asymmetric trend as a function of the sediment-entry-point location was probably induced by the selection of the well locations. The results seem to be insensitive to the initial topography. Figure 14 shows the mismatch between the lithostratigraphy at wells A, B, C, D and the probability of channel occurrence, expressed in terms of channel-volume fraction for the corresponding grid cells (Eq. 3). Again, no clear trend can be identified. Thus, differently from seismic surfaces, the hard data extracted from the reservoir (i.e. well tops and lithological logs) do not seem to be very effective for the inversion process.

Beyond giving information on the most likely values of the simulation parameters, goodness of fit functions were primarily constructed in order to reduce the uncertainty affecting the 3D channel occurrence probability (P_{CH}). This 3D channel occurrence probability was obtained as an outcome of basin simulations. In a follow-up study this information will be imposed as a soft constraint to the Kriging-like generation of reservoir realizations and will complement the constraints provided by well and seismic data. A 2D map, restricted to the reservoir domain area, of the P_{CH} values averaged over the reservoir depth is shown in figure 15a, b, and c. Figure 15a shows the P_{CH} values averaged over all the simulated scenarios; figure 15b provided the P_{CH} values averaged over a selection of the most likely scenarios (selected according to the F_{CH} and F_{top_surf} criteria applied sequentially); finally, figure 15c shows the P_{CH} values for the reference case. The comparison reveals how the selection of the most likely scenarios reduces the uncertainty related to the sandy channel occurrence.

The P_{CH} variability in the vertical direction was evaluated for the locations W1-W9, displayed in fig.16. The selected locations follow a regular pattern so as to uniformly monitor the reservoir area. The P_{CH} median value over all the considered scenarios (figure 17a) and over the 100 most likely scenarios (figure 17b) are compared to the reference case values. As it can be observed, a clear improvement of the P_{CH} median was observed when the scenarios were filtered according to the goodness of fit criteria, especially at locations W3, W6 and W9.

5 DISCUSSION AND CONCLUSIONS

Reservoir description could significantly benefit from the integration of quantitative basin-scale information into the reservoir simulation workflow. The ability to predict the occurrence and distribution of pay facies is known to be crucial during the appraisal phase of a field, when decisions have to be made based on a limited amount of available data, as well as during the field development for placement of new or infill wells. This study was aimed at demonstrating that numerical modeling of the basin-scale stratigraphy can be used to effectively steer prediction of reservoir architecture in fluvio-deltaic sedimentary environments.

The study demonstrated that accurate estimation of model input parameters, especially the initial topography and the location of the sediment entry point, is needed to achieve a reliable prediction of both the channel locations and the sand/shale volume fraction. The uncertainties associated with the input parameters strongly affected the overall channelized volume fraction as well as the elevation of the bounding surfaces and the spatial distribution of the channelized deposits.

The hard data extracted from the reservoir (i.e. well tops and lithological logs) were not very effective for the inversion process. Given that the information extracted from the basin model derived from a coarse grid and that the well data referred to a specific location in the reservoir, a direct comparison could not be made without downscaling the model output by post-processing. Inversion of the basin model based on the stratigraphic surfaces interpreted from seismic data proved to be much more successful. A clear relationship was found between the initial environmental parameters and the geometry of the bounding surfaces when the entire basin area was considered. Conversely, the inversion was much less successful when it was based on the elevation of the seismic surfaces in the reservoir area only. As a direct consequence of constraining all the realizations to the well data, the uncertainty decreased towards the well locations. Therefore, all the initial topographies were subject to less uncertainty in the reservoir area than in the surrounding area and did not contain much information on stratigraphic variability. Similarly, the modelled top stratigraphic surfaces are less sensitive to initial topography if restricted to the reservoir area. This result clearly showed that attempts to fit (geostatistical) reservoir models to local data only, which happens to be the standard workflow in reservoir modeling, might not be the most successful approach to constraining reservoir models. Regional seismic surveys, which are commonly available in the appraisal phase, provide a wealth of information on the area surrounding the targeted reservoir volume, effectively acting as boundary conditions for the reservoir model. Thus, the definition of a correct velocity model to minimize the uncertainty of the time-to-depth conversion has a significant impact on the accuracy of the stratigraphic inversion. If the uncertainties associated with the initial and boundary conditions of basin-scale simulations can be significantly reduced, the lithostratigraphic record generated by the sub-grid parameterization can be used to predict the spatial distribution of lithology at the reservoir scale through application of appropriate geostatistical post-processing tools such as multipoint statistics (Daly and Caers, 2010). This will be the subject of a follow-up study.

APPENDIX

The function F_{well_top} measuring the well-top misfit was defined as follows:

$$F_{well\_top} = \frac{1}{n_{wells}} \sqrt{\sum_{iw=1}^{n_{wells}} \frac{\left| z_{top\,iw} - \bar{z}_{top\,iw} \right|^2}{\bar{z}_{top\,iw}}} \tag{2}$$

where $z_{top\,iw}$ and $\bar{z}_{top\,iw}$ are the elevation of the final topography at the iw^{th} well estimated from simulation and log, respectively, and n_{wells} is the number of wells.

The function F_{CH} measuring the mismatch between the evidence of channel facies from well logs and the corresponding *channel occurrence probability* (P_{CH}) from simulated results is expressed by the sum of two terms; the first term expresses the fraction of depth point in which P_{CH} =0 but well log exhibit channel (R=1) and the second the fraction of depth point in which P_{CH} =1 but well log exhibit floodplain (non-channel, R=0):

$$F_{CH} = \frac{1}{n_{wells}} \sum_{iw=1}^{n_{wells}} \left(\frac{1}{2} \left(\frac{1}{nz_{iiw}} \sqrt{\sum_{z_i} \left(R_{iw}(z_i) = CH \right)^2} + \frac{1}{nz_{jiw}} \sqrt{\sum_{z_j} \left(R_{iw}(z_j) \neq CH \right)^2} \right) \right), where\, z_i \mid P_{CHiw}(z_i) = 0,\; z_j \mid P_{CHiw}(z_j) = 1 \tag{3}$$

where $R_{iw}(z_i)$ is the lithology of well *iw* at the quote z_i, CH is the channel lithology, $P_{CHiw}(z_i)$ is the channel volume fraction of the grid cell intercepting the iw^{th} well at the depth z_i; nz_{iiw} is the number of depth points of the iw^{th} well that are expected for sure not to intercept a channel $\left(P_{CHiw}(z_i) = 0\right)$, analogously nz_{jiw} is the number of depth points of the iw^{th} well that are expected for sure to intercept a channel $\left(P_{CHiw}(z_j) = 1\right)$. The channel-occurrence probability for each well $P_{CHiw}(z_{ifp})$ is calculated as follows:

$$P_{CHiw}(z_{ifp}) = \frac{V_{CH}}{V_{cell}} \tag{4}$$

where V_{CH} is the channel volume in the grid cell containing the well *iw* at the depth z_{ifp} corresponding to the intercepted floodplain *ifp*, and V_{cell} represents the cell volume of the corresponding grid. The channel occurrence probability is assumed to be constant along the channel thickness (h). The latter is estimated from the channel volume, given the thickness-to-width ratio (f):

$$h(x,y,z)=\sqrt{\frac{V_{CH}\cdot f}{l_{CH}}} \tag{5}$$

where the channel length l_{CH} is approximated with the cell dimension Δx . The thickness-to-width ratio was chosen as 1/250, according to Reynolds (1999).

The goodness of fit function F_{top_surf} measures the mismatch between the simulated and the seismic top surfaces, accounting for uncertainty on seismic data through a tolerance interval for the top surface.

It reads:

$$F_{top\_surf}=\frac{1}{\sqrt{n_x n_y}\sqrt{\sigma^2\left(z_{top\_surf}\right)}}\sqrt{\sum_{i,j} d\left(x_i,y_i\right)^2} \tag{6}$$

where $n_x n_y$ is the number of cells of the grid covering the area; $\sigma^2\left(z_{top\_surf}\right)$ is the variance among depth data of the top surface and $d\left(x_i,y_i\right)$ is the punctual distance between surfaces, computed as:

$$d\left(x_i,y_i\right)=Max\left(\left|z_{top\_surf}(x_i,y_i)-z_{ref\_surf}(x_i,y_i)\right|-toll,0\right) \tag{7}$$

where $z_{top\_surf}(x_i,y_i)$ is the elevation of the final topography in the cell corresponding to the coordinates x_i,y_i and *toll* is the tolerance interval.

References

AMAEFULE, J.O. , KEELAN, D.K. (1989): Stochastic Approach to computation of Uncertainties in Petrophysical Parameters, Soc. of Core Analysts, No. SCA-8907.

BENTLEY, M., SMITH, S. (2008). Scenario-based reservoir modelling: The need for more determinism and less anchoring. In: Robinson, A., Griffiths, P., Price, S., Hegre, J., Muggeridge, A. (eds.), The Future Of Geological Modelling In Hydrocarbon Development. Geological Society (London) Special Publication 309, p. 145–159.

BORNHOLDT, S., NORDLUND, U., WESTPHAL, H. (1999). Inverse stratigraphic modelling using genetic algorithms. In: Harbaugh, J.W., Watney, W.L., Rankey, E.C., Slingerland, R., Goldstein, R.H., Franseen, E.K. (eds.), Numerical Experiments In Stratigraphy: Recent Advances In Stratigraphic And Sedimentologic Computer Simulations, SEPM Special Publication 62, p. 85–90.

BOSCHETTI, F. , MORESI, L. 2001. Interactive inversion in geosciences. Geophysics, 66 (4), 1226–1234.

BOWMAN, S.A., VAIL, P.R. (1999). Interpreting the stratigraphy of the Baltimore canyon section, offshore New Jersey with PHIL, a stratigraphic simulator. In: Harbaugh, J.W., Watney, W.L., Rankey, E.C., Slingerland, R., Goldstein, R.H., Franseen, E.K. (eds.), Numerical Experiments In Stratigraphy: Recent Advances In Stratigraphic And Sedimentologic Computer Simulations, SEPM Special Publication 62, p. 117-138.

BURGESS P.M. (2012). A brief review of developments in stratigraphic forward modelling, 2000-2009. In Roberts, D.G., Bally, A.W. (eds.), Regional Geology And Tectonics: Principles Of Geologic Analysis, Elsevier. DOI: 10.1016/B978-0-444-53042-4.00014-5

BURGESS, P.M. (2001). Modelling carbonate sequence development without relative sealevel oscillations. Geology, 29, 1127-1130.

BURGESS, P.M., LAMMERS, H.M., VAN OOSTERHOUT, C., GRANJEON, D. (2006). Multivariate sequence stratigraphy: tackling complexity and uncertainty with stratigraphic forward modeling, multiple scenarios and conditional frequency maps. AAPG Bulletin, 90, 1883-1901.

BURTON, R., KENDALL, C.G.ST.C., LERCHE, I. (1987). Out of our depth: On the impossibility of fathoming eustasy from the stratigraphic record. Earth-Science Reviews, 24, 237–277.

CAFLISCH, R. E. (1998). Monte Carlo and quasi-Monte Carlo methods, Acta Numerica, 7, 1-49.

CHARVIN, K, HAMPSON, G.J., GALLAGHER, K.L., STORMS, J.E.A., LABOURDETTE, R. (2011). Characterization of controls on high-resolution stratigraphic architecture in wave-dominated shoreface–shelf parasequences using inverse numerical modeling. Journal of Sedimentary Research, 81, 562–578.

CHARVIN, K., GALLAGHER, K.L., HAMPSON, G., LABOURDETTE, R. (2009). A Bayesian approach to inverse modeling of stratigraphy, part 1: method. Basin Research, 21, 5–25.

CLEVIS, Q., DE BOER, P.L., WACHTER, P.M. (2003). Numerical modelling of drainage basin evolution and three-dimensional alluvial fan stratigraphy. Sedimentary Geology, 163, 85-110.

COCHRAN, W.G. (1963). Sampling Techniques. John Wiley & Sons Inc., New York.

CROSS, T.A., LESSENGER, M. (1999). Construction and application of stratigraphic inverse model. In: Harbaugh, J.W., Watney, W.L., Rankey, E.C., Slingerland, R., Goldstein, R.H., Franseen, E.K. (eds.), Numerical Experiments In Stratigraphy: Recent Advances In Stratigraphic And Sedimentologic Computer Simulations, SEPM Special Publication 62, p. 69-83.

DALMAN, R.A.F., WELTJE, G.J. (2008). Sub-grid parameterisation of fluvio-deltaic processes and architecture in a basin-scale stratigraphic model. Computers and Geosciences, 34, 1370– 1380.

DALMAN, R.A.F., WELTJE, G.J. (2012). SimClast: an aggregated forward stratigraphic model of continental shelves. Computers and Geosciences, 38, 115-126.

DALY, C., CAERS, J. (2010). Multi-point geostatistics – an introductory overview. First break, 28, 39–47.

DEUTSCH, C.V. (2002). Geostatistical Reservoir Modeling. Oxford University Press, Oxford.

DEVEUGLE, P.E.K., JACKSON, M.D., HAMPSON, G.J., STEWART, J., CLOUGH, M.D., EHIGHEBOLO, T., FARRELL, M.E., CALVERT, C.S., MILLER, J.K. (2014). A comparative study of reservoir modeling techniques and their impact on predicted performance of fluvial-dominated deltaic reservoirs. AAPG Bulletin, 98, 729–763.

DOLIGEZ, B., GRANJEON, D., JOSEPH, P., ESCHARD, R., BEUCHER, H. (1999) How can stratigraphic forward modelling help to constrain geostatistical reservoir simulations? In: Harbaugh, J.W., Watney, W.L., Rankey, E.C., Slingerland, R., Goldstein, R.H., Franseen, E.K. (eds.), Numerical Experiments In Stratigraphy: Recent Advances In Stratigraphic And Sedimentologic Computer Simulations, SEPM Special Publication 62, p. 239-244.

FALIVENE, O., FRASCATI, A., GESBERT, S., PICKENS, J., HSU, Y., ROVIRA, A. (2014). Automatic calibration of stratigraphic forward models for predicting reservoir presence in exploration. AAPG Bulletin, 98, 1811–1835.

GRANJEON, D., JOSEPH, P. (1999). Concepts and applications of a 3-D multiple lithology, diffusive model in stratigraphic modeling. In: Harbaugh, J.W., Watney, W.L., Rankey, E.C., Slingerland, R., Goldstein, R.H., Franseen, E.K. (eds.), Numerical Experiments In Stratigraphy: Recent Advances In Stratigraphic And Sedimentologic Computer Simulations, SEPM Special Publication 62, p. 197– 210.

GRIFFITHS, C.M., DYT, C., PARASCHIVOIU, E., LIU, K. (2001). SEDSIM in hydrocarbon exploration. In: Merriam, D., Davis, J.C. (eds), Geological Modeling And Simulation. Kluwer Academic, New York.

HASTIE, T., TIBSHIRANI, R., FRIEDMAN, J. (2009). The Elements Of Statistical Learning: Data Mining, Inference, and Prediction, Second Edition, Springer, New York.

HELLER, P.L., BURNS, B.A., MARZO, M. (1993). Stratigraphic solution sets for determining the roles of sediment supply, subsidence, and sea level on transgressions and regressions. Geology, 21, 747-750.

HUTTON, E.W.H, SYVITSKI, J.P.M. (2008). SedFlux 2.0: an advanced process response model that generates 3-D stratigraphy. Computers and Geosciences, 34, 1319–1337.

IMHOF, M. G., SHARMA, A.K. (2006). Quantitative seismostratigraphic inversion of a prograding delta from seismic data. Marine and Petroleum Geology, 23, 735–744.

JCGM (2008). Evaluation of measurement data - Supplement 1 to the “guide to the expression of uncertainty in measurement” - propagation of distributions using a Monte Carlo method. Joint Committee for Guides in Metrology, JCGM 101:2008.

KARSSENBERG, D., DE VRIES, M., BRIDGE, J.S. (2007). Conditioning a process-based fluvial-stratigraphy model to well data by inverse estimation of model inputs using genetic algorithm. AAPG Search and Discovery article #90063, AAPG Annual Convention, Long Beach, California.

KARSSENBERG, D., TORNQVIST, T., BRIDGE, J. S. (2001). Conditioning a process-based model of sedimentary architecture to well data. Journal of Sedimentary Research, 71, 868-879.

LERCHE, I. (1992) Oil Exploration: Basin Analysis and Economics, Academic Press, San Diego.

LERCHE, I. (1996) An inverse method for determining parameters for folded structures. Quarterly of Applied Mathematics, 54, 625-636.

LESSENGER, M., CROSS T.A., 1996, An Inverse Stratigraphic Simulation Model - Is Stratigraphic Inversion Possible?: Energy Exploration Exploitation, v. 14, p. 627-637.

MEIJER, X. D. (2002). Modeling the drainage evolution of a river-shelf system forced by Quaternary glacio-eustasy. Basin Research, 14, 361-337.

MENEVEAU, C. (2010). Turbulence: subgrid-scale modeling. Scholarpedia, 5(1): 9489 (DOI:10.4249/scholarpedia.9489).

NAKAYAMA, K. (2000): Estimation of Reservoir Properties by MonteCarlo Simulation, SPE, 59408

NAVAL, B. (2009). Business Statistics, Pearson Education, New Delhi.

PAL, S.K. (1998). Statistics For Geoscientists - Techniques And Applications. Concept Publishing Company, New Delhi.

PAOLA, C. (2000). Quantitative models of sedimentary basin filling, Sedimentology, 47 (Suppl. 1), 121-178.

REYNOLDS, A.D. (1999) Dimensions of paralic sandstone bodies. AAPG Bulletin, 83, 211–229.

STORMS J.E.A., WELTJE, G.J., VAN DIJKE J.J., GEEL, C.R., KROONENBERG S.B. (2002). Process-response modeling of wave-dominated coastal systems: simulating evolution and stratigraphy on geological time scales. Journal of Sedimentary Research, 72, 226-239.

TAYLOR, J.R., (1982), An Introduction to Error Analysis. The study of uncertainties in physical measurements. University Science Books, Sausalito, California.

TETZLAFF, D.M., HARBAUGH, J.W. (1989). Simulating Clastic Sedimentation. Computer Methods In The Geosciences, Van Nostrand Reinhold, New York.

VERGA, F., CANCELLIERE M., VIBERTI, D. (2013). Improved application of assisted history matching techniques. Journal of Petroleum Science and Engineering, 109, 327-347.

VIBERTI, D., VERGA, F. (2012). An approach for the reliable evaluation of the uncertainties associated to petrophysical properties. Mathematical Geosciences, 44, 327-341.

WARD, J.H. (1963). Hierarchical grouping to optimize an objective function. Journal of the American Statistical Association 58, 236–244.

WARNER, J.C., SHERWOOD, C.R., SIGNELL, R.P., HARRIS, C.K., ARANGO, H.G. (2008). Development of a three-dimensional, regional, coupled wave, current, and sediment-transport model. Computers and Geosciences, 34, 1284-1306.

WARRLICH, G.M.D., BOSENCE, D., WALTHAM, D., WOOD, C., BOYLAN, A., BADENAS, B., (2008). 3D stratigraphic forward modeling for analysis and prediction of carbonate platform stratigraphies in exploration and production. Marine and Petroleum Geology, 25, 35-58.

WELTJE, G.J., DALMAN, R.A.F., KARAMITOPOULOS, P., SACCHI, Q. (2013). Reducing the uncertainty of static reservoir models: implementation of basin-scale geological constraints. SPE-164821-MS.

WENDEBOURG, J., HARBAUGH, J.W. (1997). Simulating Oil Entrapment in Clastic Sequences. Pergamon Press, Oxford.

WIJNS, C., POULET, T., BOSCHETTI, F., DYT, C., GRIFFITHS, C.M. (2004) Interactive inverse methodology applied to stratigraphic forward modelling. In: Curtis, A., Wood, R. (eds.), Geological Prior Information: Informing Science And Engineering, Geological Society (London), Spec. Publ. 239, pp. 147-156.

FIGURE CAPTIONS

Fig. 1: 3D view of basin-scale model in terms of net to gross and fluvial architecture at reservoir scale. Reference wells A to D are also displayed.

Fig. 2: Stratigraphy at wells A, B, C, D. Top and bottom surfaces are displayed as dotted lines.

Fig. 3: Realizations of the initial topography with well locations (A, B, C, D) and outline of reservoir zone (white rectangle).

Fig. 4: Goodness of fit of initial topographies with respect to the seismic data of the reference case.

Fig. 5: Locations of possible sediment entry points and range of sea levels considered in the study.

Fig. 6: Channelized volume fraction (%) in the reservoir zone. Initial topographies are ranked according to similarity to reference case.

Fig. 7: Histograms of the (a) sand fraction (%) and (b) channel directions in the reservoir zone based on the basin-scale model.

Fig. 8: Dendrogram (a) and cluster analysis (b) of the considered scenarios based on the basin stratigraphy. The cut was selected at the level maximizing the distance between clusters.

Fig. 9: Dendrogram (a) and cluster analysis (b) of the considered scenarios based on the 3D map of channel occurrence probability. The cut was selected at the level maximizing the distance between clusters.

Fig. 10: Goodness of fit of the basin scenarios based on the top stratigraphic surface (F_{top_surf}) across the whole basin area: all scenarios (a) and 100/2000 most likely scenarios (b).

Fig. 11: Goodness of fit of the basin scenarios based on the top stratigraphic surface (F_{top_surf}) restricted to the reservoir zone: all scenarios (a) and 100/2000 most likely scenarios (b).

Fig. 12: Distribution of the goodness of fit function F_{top_surf} based on the mismatch of the top stratigraphic surface across the whole basin area (a) and for the reservoir area only (b).

Fig. 13: Goodness of fit of the basin scenarios based on the well tops (F_{well_top}) at wells A, B, C, D: all scenarios (a) and 100/2000 most likely scenarios (b).

Fig. 14: Goodness of fit of the basin scenarios based on the lithological similarities (F_{CH}) at wells A, B, C, D: all scenarios (a) and 100/2000 most likely scenarios (b).

Fig. 15: Reduction of uncertainty over channel occurrence probability (P_{CH}): average over all scenarios (a), average over a subset of selected scenarios (b), reference case (c). P_{CH} values shown in 2D map corresponding to the reservoir area are depth-averaged.

Fig. 16: 3D distribution of Channel Occurrence Probability in the reservoir area (Reference case) with monitoring locations (W1-W9) displayed.

Fig. 17: Reduction of uncertainty over channel occurrence probability (P_{CH}) at basin scale at selected monitoring locations (W1-W9): all scenarios (a) and 100/2000 most likely scenarios (b), where F_{CH} and F_{top_surf} criteria were sequentially applied.

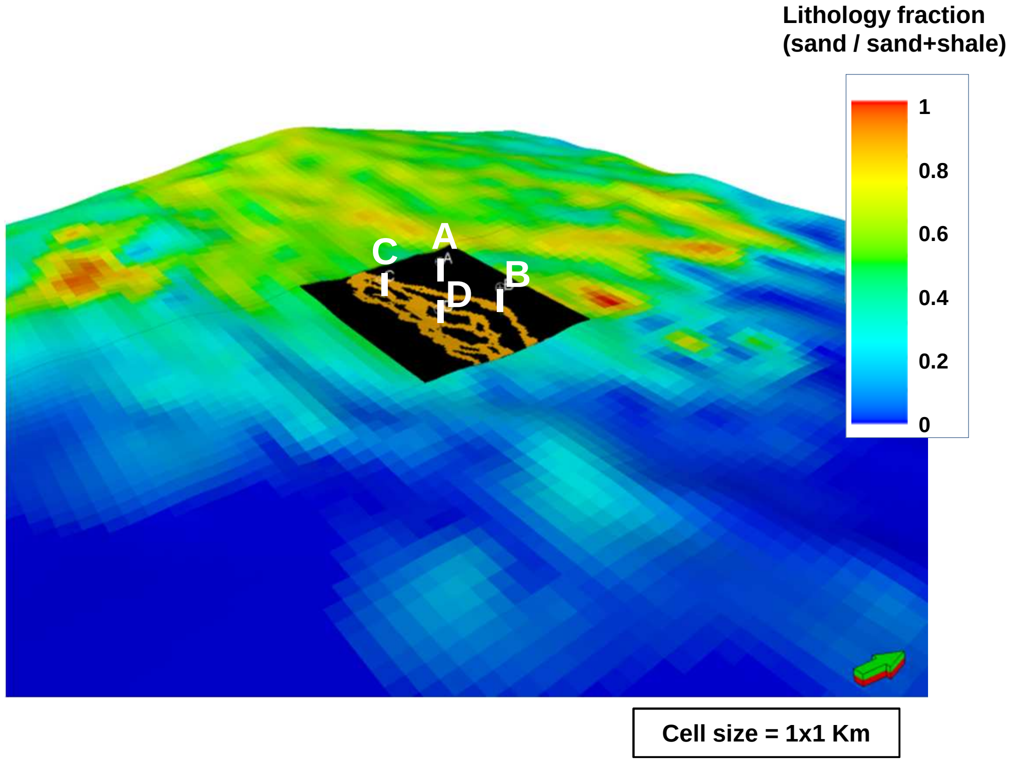
Lithology fraction
(sand / sand+shale)
1
0.8
0.6
0.4
0.2
0
A
B
C
D
Cell size = 1x1 Km

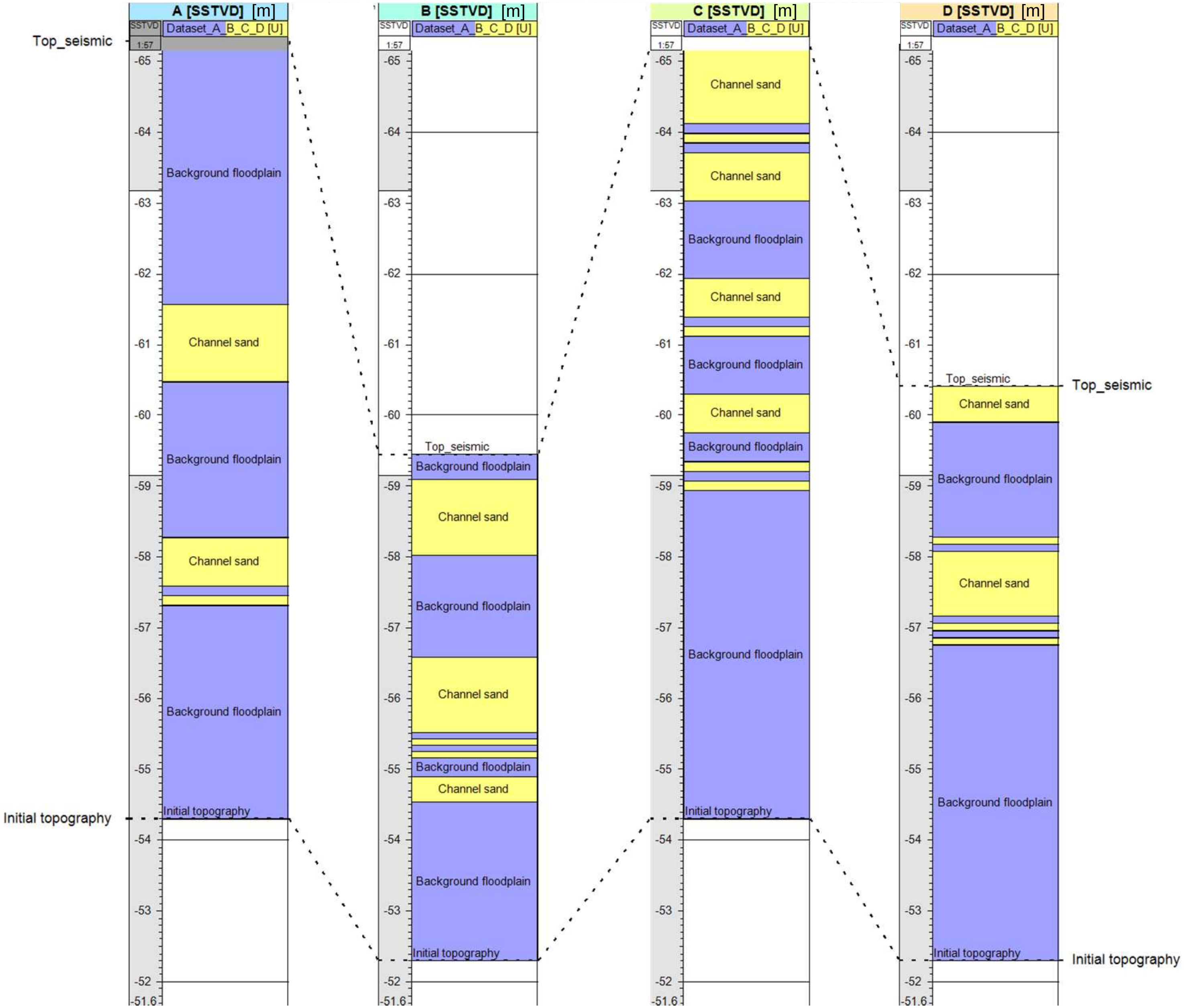

A [SSTVD] [m]
B [SSTVD] [m]
C [SSTVD] [m]
D [SSTVD] [m]
Dataset_A_B_C_D [U]
Top_seismic
Initial topography
Background floodplain
Channel sand
-65
-64
-63
-62
-61
-60
-59
-58
-57
-56
-55
-54
-53
-52
-51.6

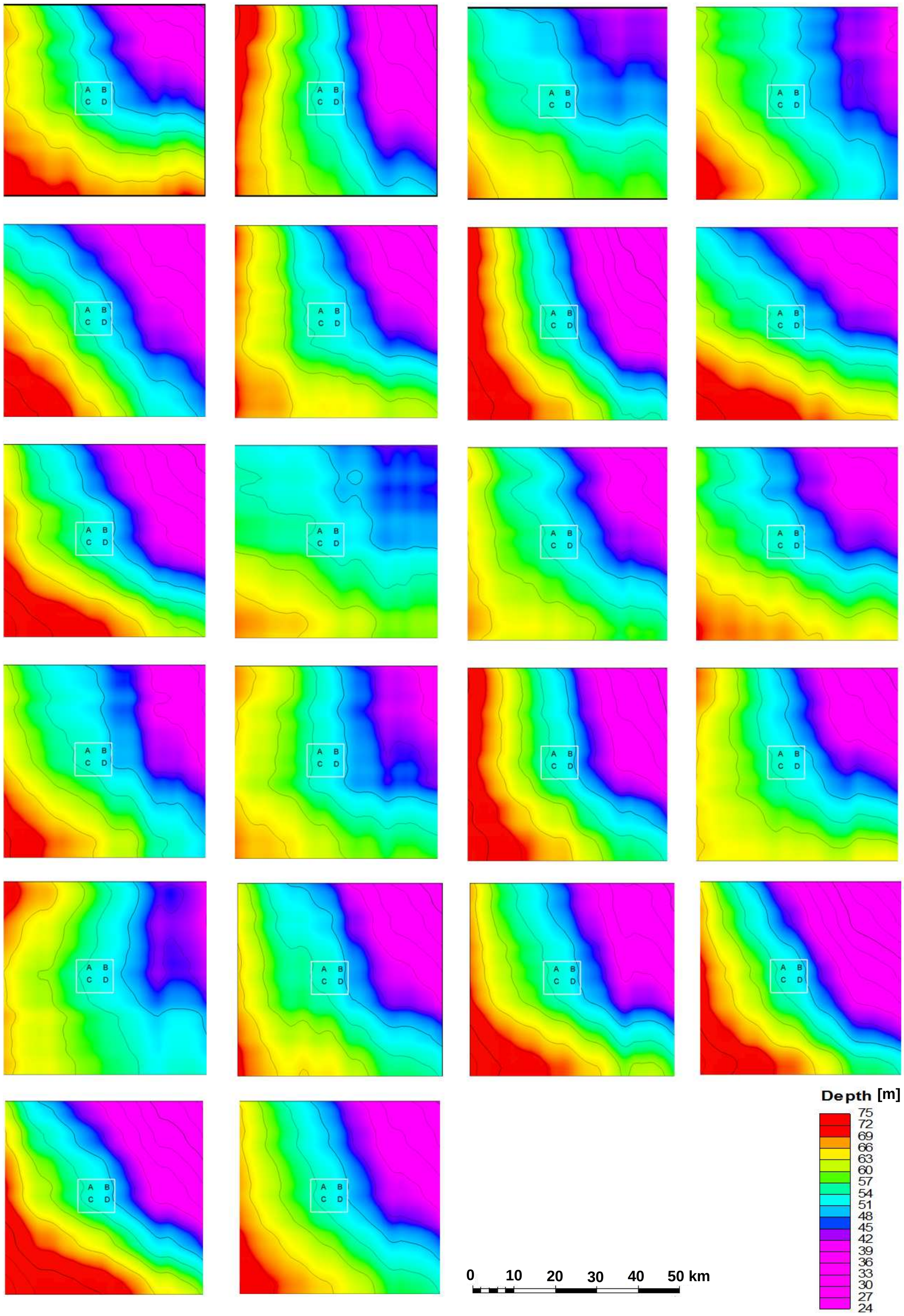
A B
C D
0 10 20 30 40 50 km
Depth [m]
75
72
69
66
63
60
57
54
51
48
45
42
39
36
33
30
27
24

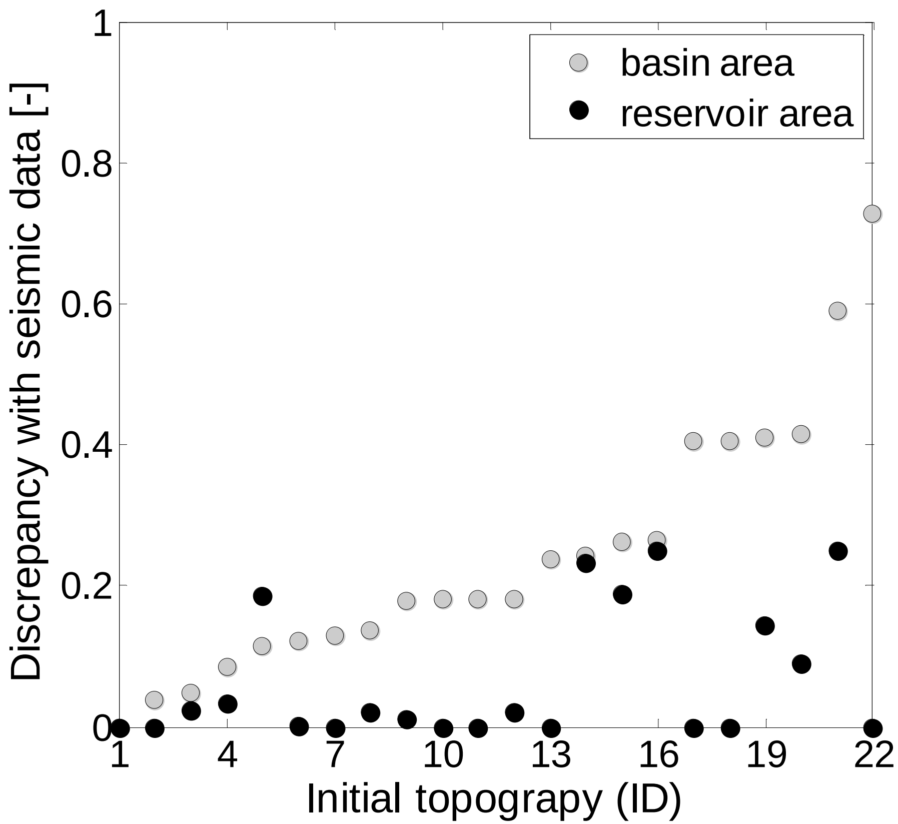

basin area
reservoir area
Discrepancy with seismic data [-]
0
0.2
0.4
0.6
0.8
1
1
4
7
10
13
16
19
22
Initial topograpy (ID)

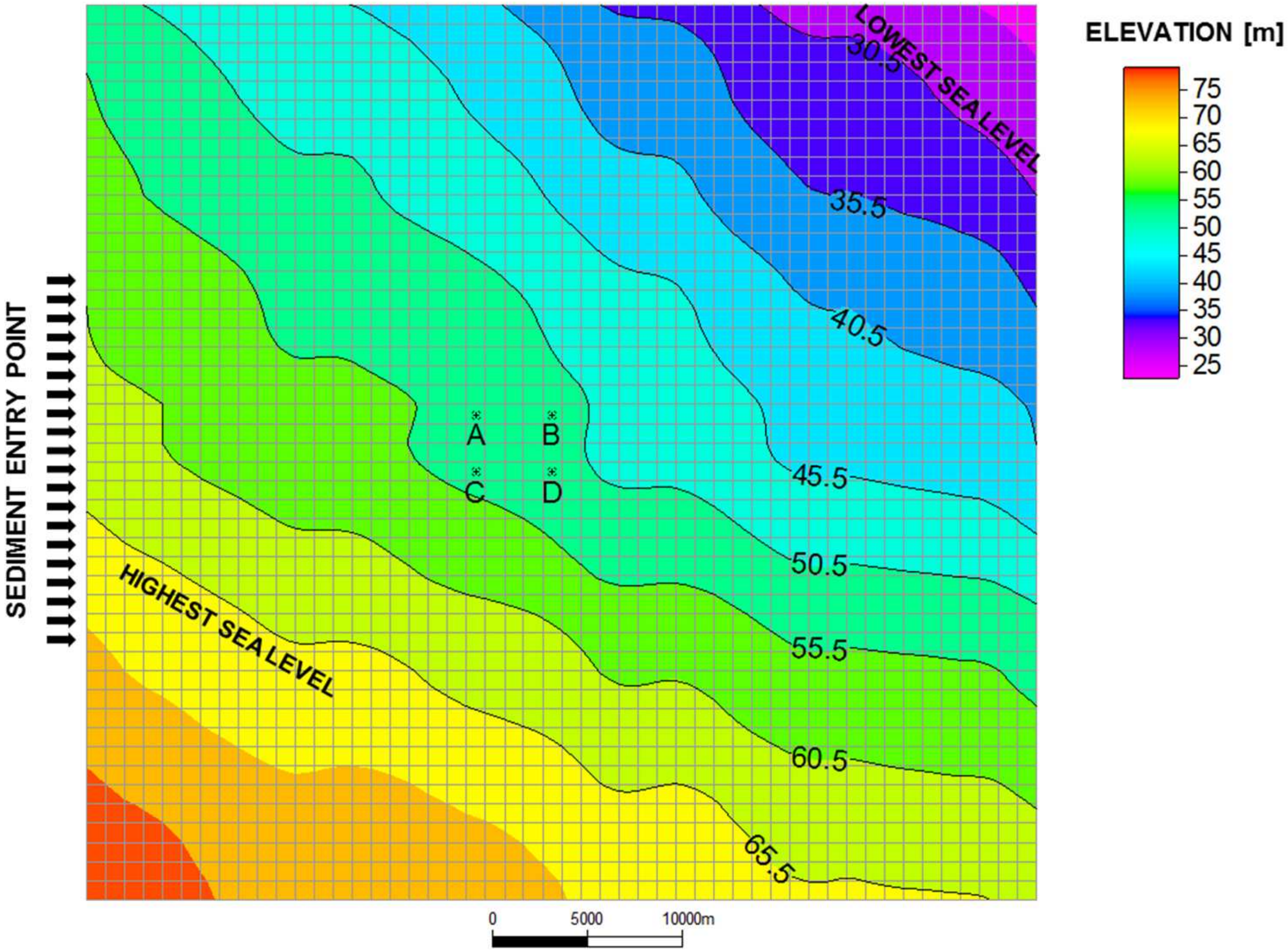
ELEVATION [m]
75
70
65
60
55
50
45
40
35
30
25
LOWEST SEA LEVEL
HIGHEST SEA LEVEL
SEDIMENT ENTRY POINT
30.5
35.5
40.5
45.5
50.5
55.5
60.5
65.5
A
B
C
D
0
5000
10000m

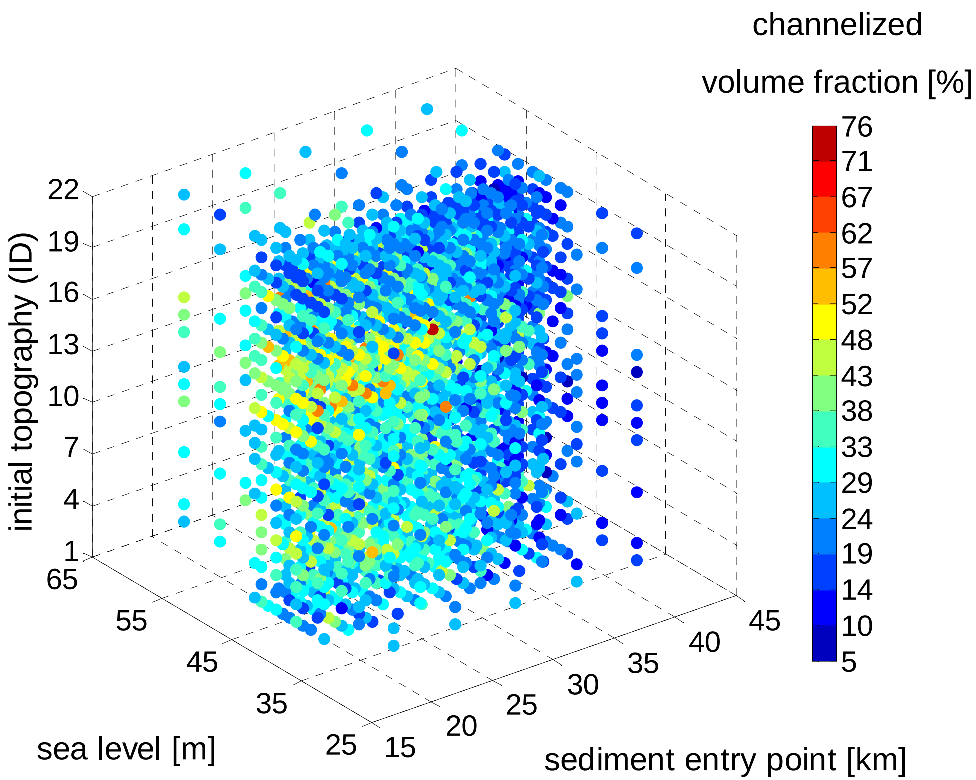
channelized
volume fraction [%]
76
71
67
62
57
52
48
43
38
33
29
24
19
14
10
5
initial topography (ID)
22
19
16
13
10
7
4
1
65
55
45
35
25
sea level [m]
15
20
25
30
35
40
45
sediment entry point [km]

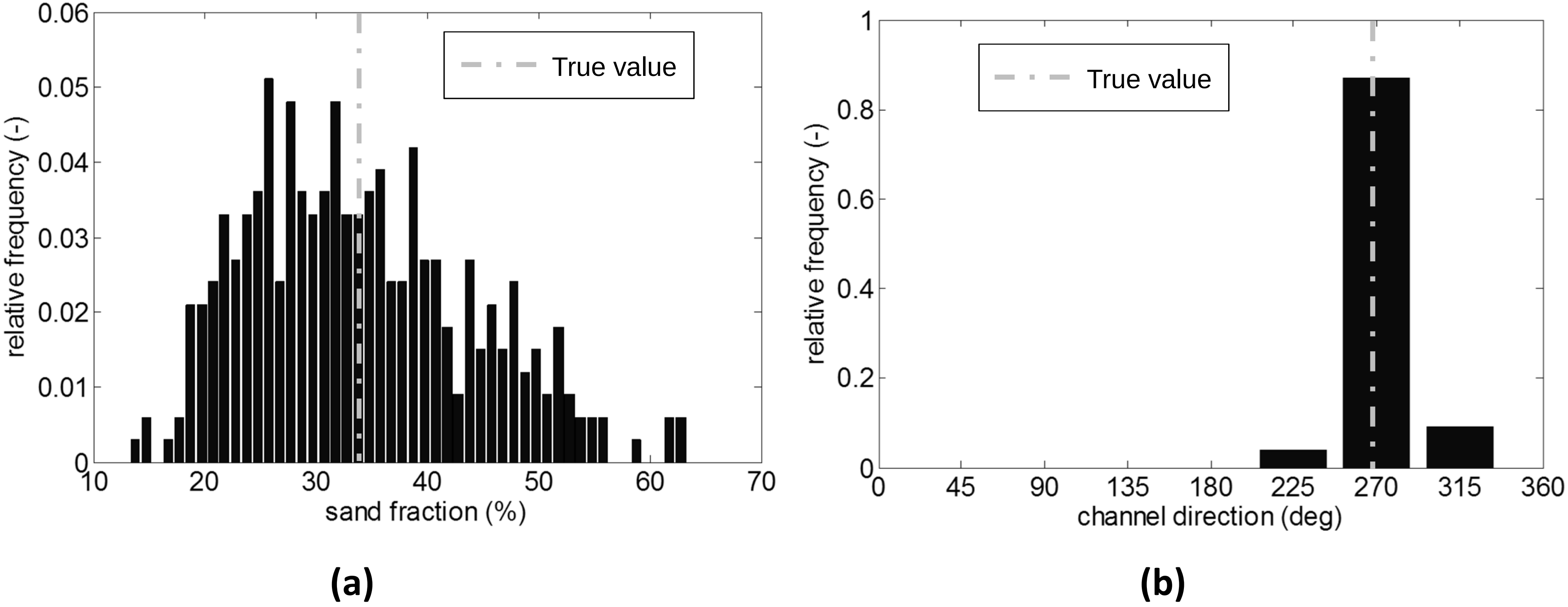
0.06
0.05
0.04
0.03
0.02
0.01
0
relative frequency (-)
True value
10
20
30
40
50
60
70
sand fraction (%)
(a)
1
0.8
0.6
0.4
0.2
0
relative frequency (-)
True value
0
45
90
135
180
225
270
315
360
channel direction (deg)
(b)

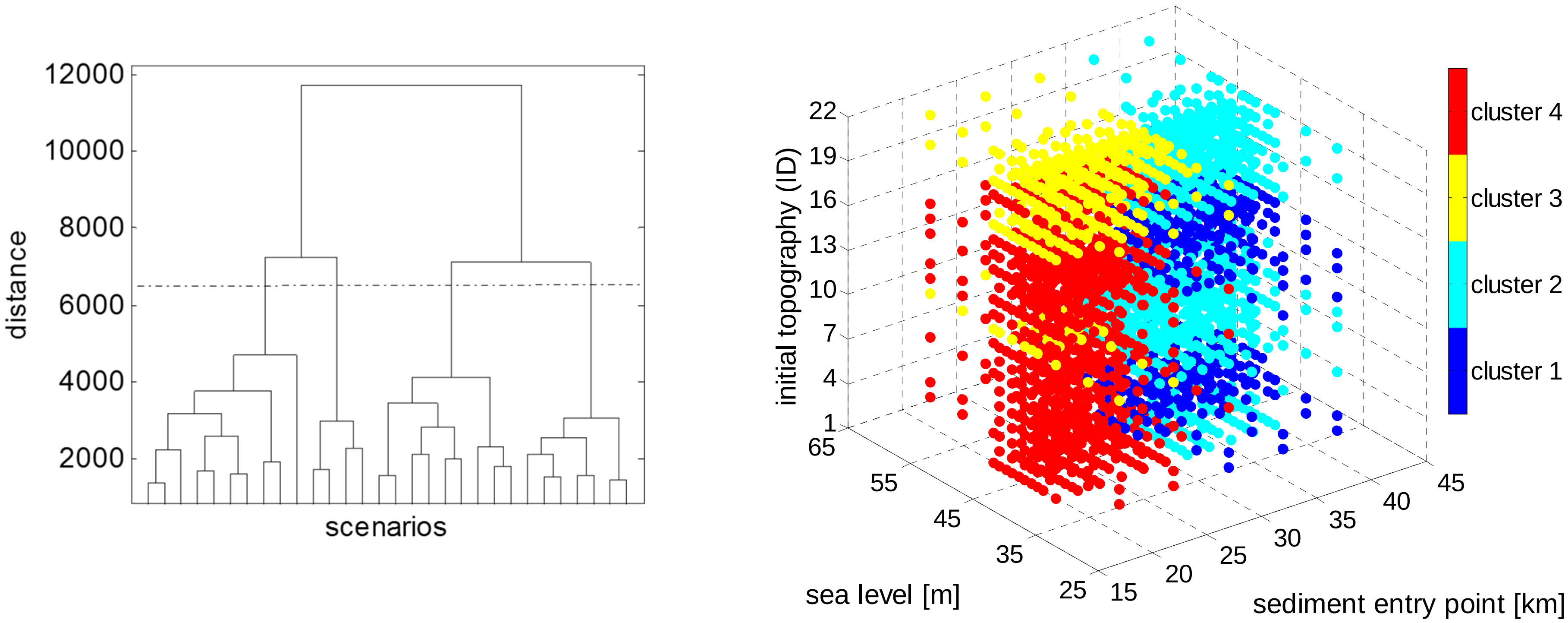
12000
10000
8000
6000
4000
2000
distance
scenarios
initial topography (ID)
22
19
16
13
10
7
4
1
65
55
45
35
25
sea level [m]
15
20
25
30
35
40
45
sediment entry point [km]
cluster 4
cluster 3
cluster 2
cluster 1

(a) **(b)**

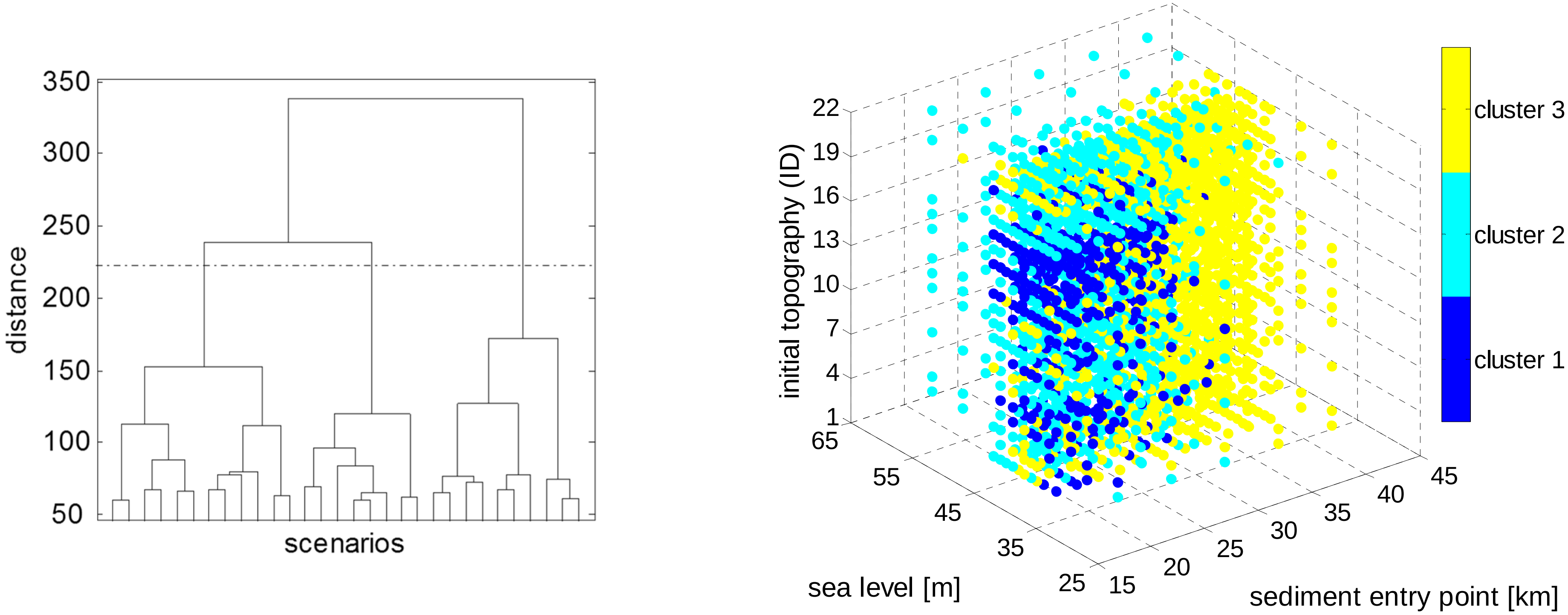

350
300
250
200
150
100
50
distance
scenarios
22
19
16
13
10
7
4
1
initial topography (ID)
65
55
45
35
25
sea level [m]
15
20
25
30
35
40
45
sediment entry point [km]
cluster 3
cluster 2
cluster 1

(a) **(b)**

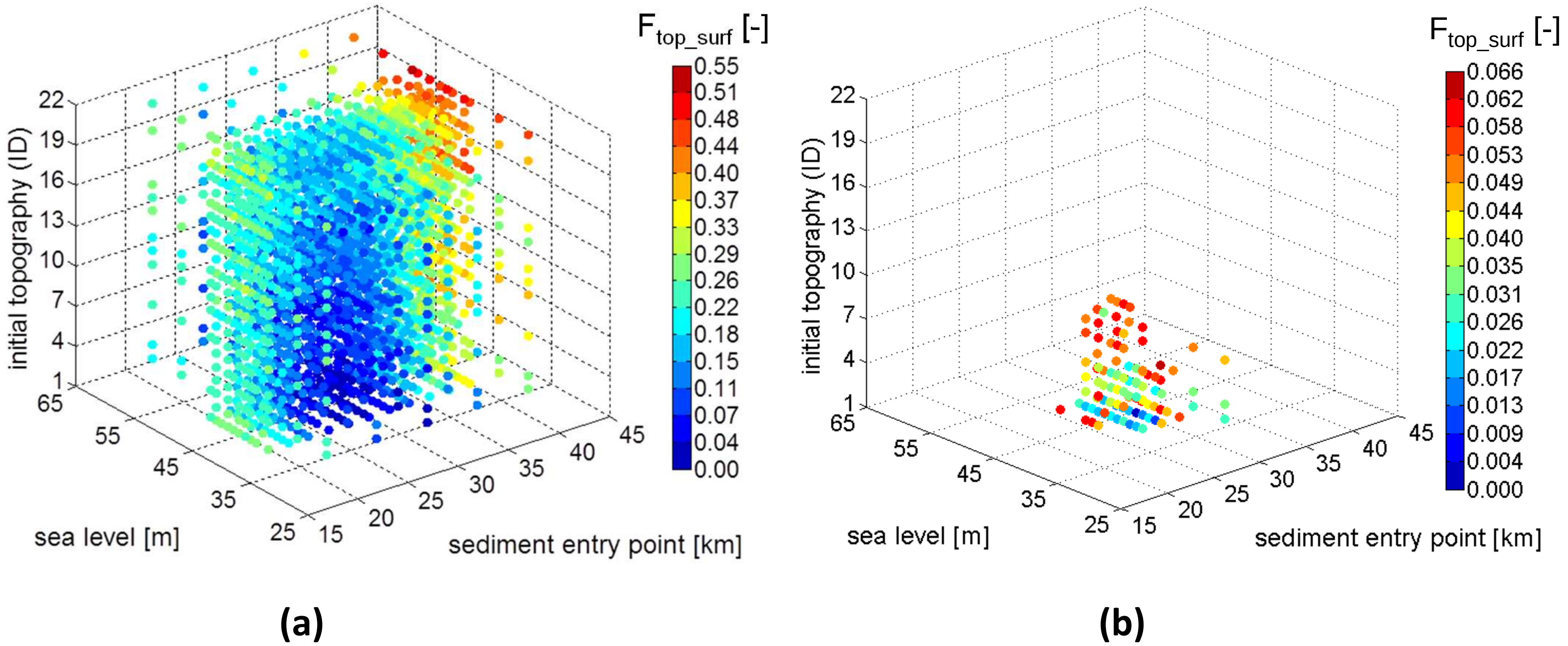
F_top_surf [-]
0.55
0.51
0.48
0.44
0.40
0.37
0.33
0.29
0.26
0.22
0.18
0.15
0.11
0.07
0.04
0.00
initial topography (ID)
22
19
16
13
10
7
4
1
sea level [m]
65
55
45
35
25
sediment entry point [km]
15
20
25
30
35
40
45
(a)
F_top_surf [-]
0.066
0.062
0.058
0.053
0.049
0.044
0.040
0.035
0.031
0.026
0.022
0.017
0.013
0.009
0.004
0.000
initial topography (ID)
sea level [m]
sediment entry point [km]
(b)

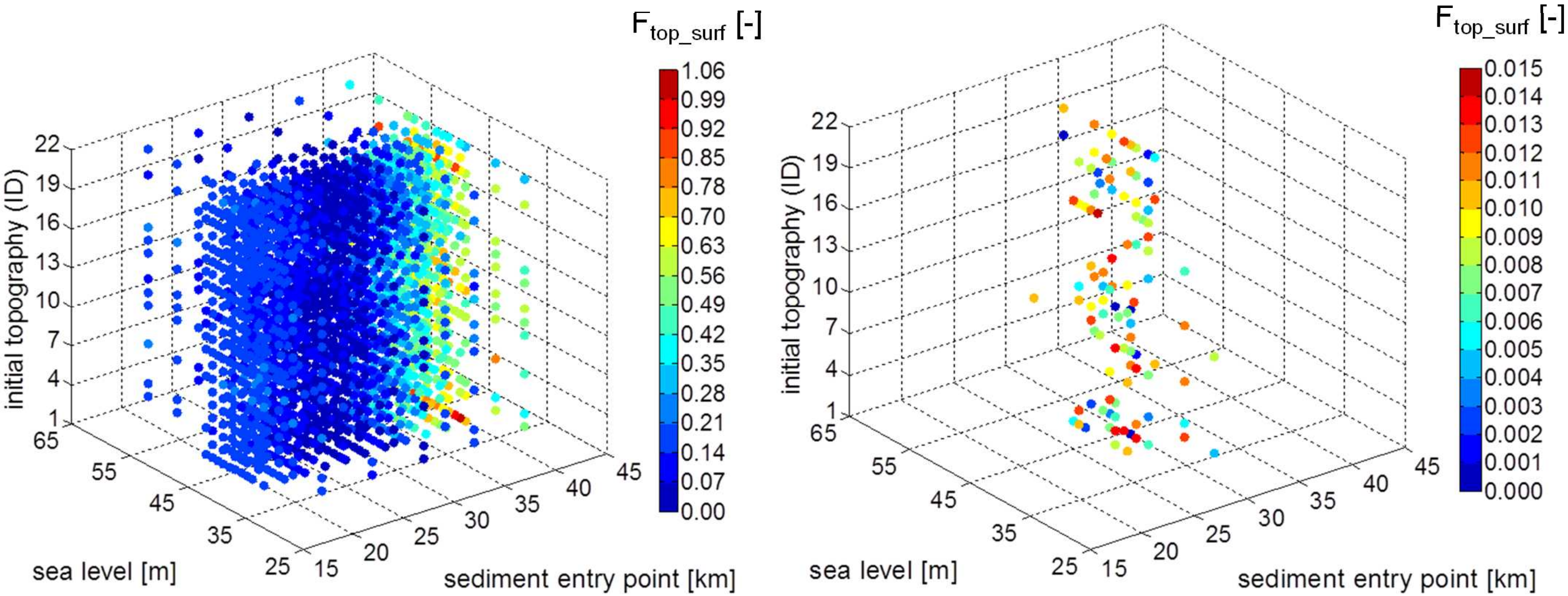

F_top_surf [-]
1.06
0.99
0.92
0.85
0.78
0.70
0.63
0.56
0.49
0.42
0.35
0.28
0.21
0.14
0.07
0.00
initial topography (ID)
sea level [m]
sediment entry point [km]
F_top_surf [-]
0.015
0.014
0.013
0.012
0.011
0.010
0.009
0.008
0.007
0.006
0.005
0.004
0.003
0.002
0.001
0.000
initial topography (ID)
sea level [m]
sediment entry point [km]

(a) **(b)**

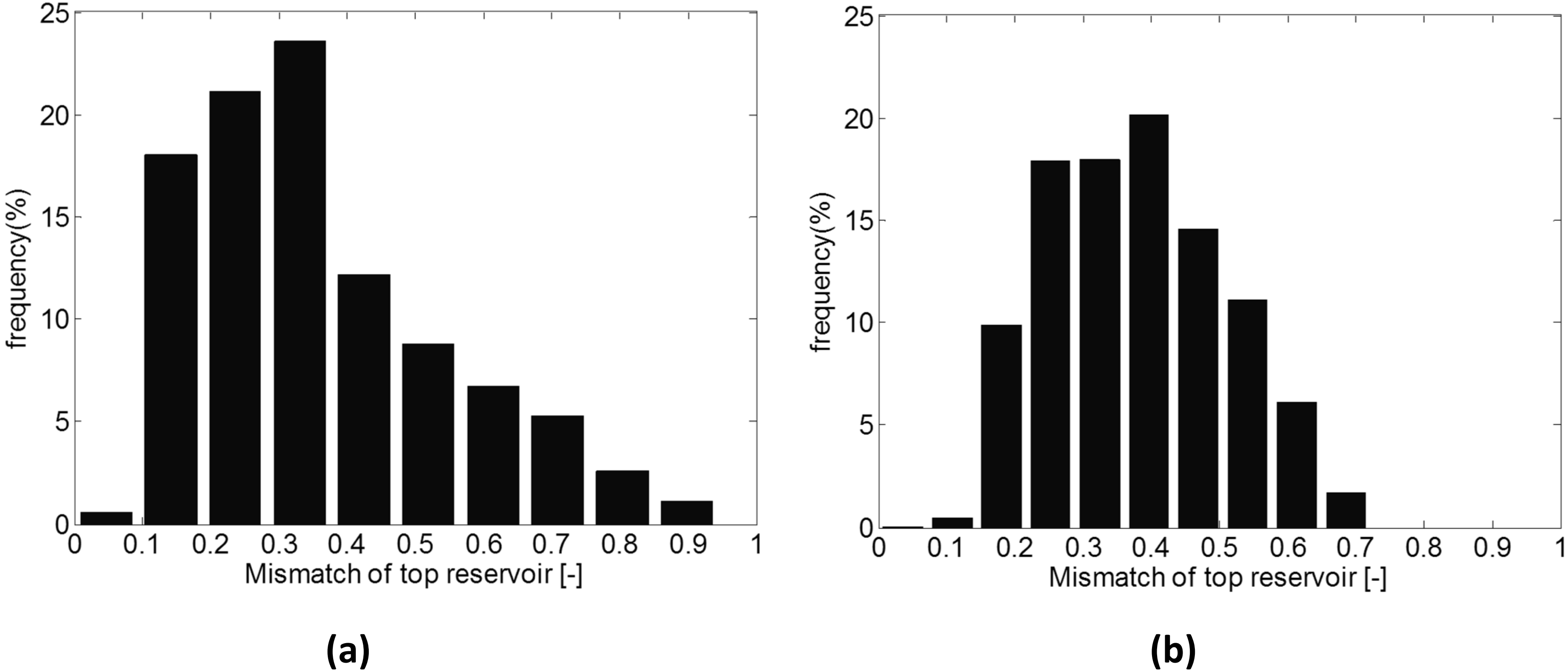

25
20
15
10
5
0
frequency(%)
0
0.1
0.2
0.3
0.4
0.5
0.6
0.7
0.8
0.9
1
Mismatch of top reservoir [-]
(a)
25
20
15
10
5
0
frequency(%)
0
0.1
0.2
0.3
0.4
0.5
0.6
0.7
0.8
0.9
1
Mismatch of top reservoir [-]
(b)

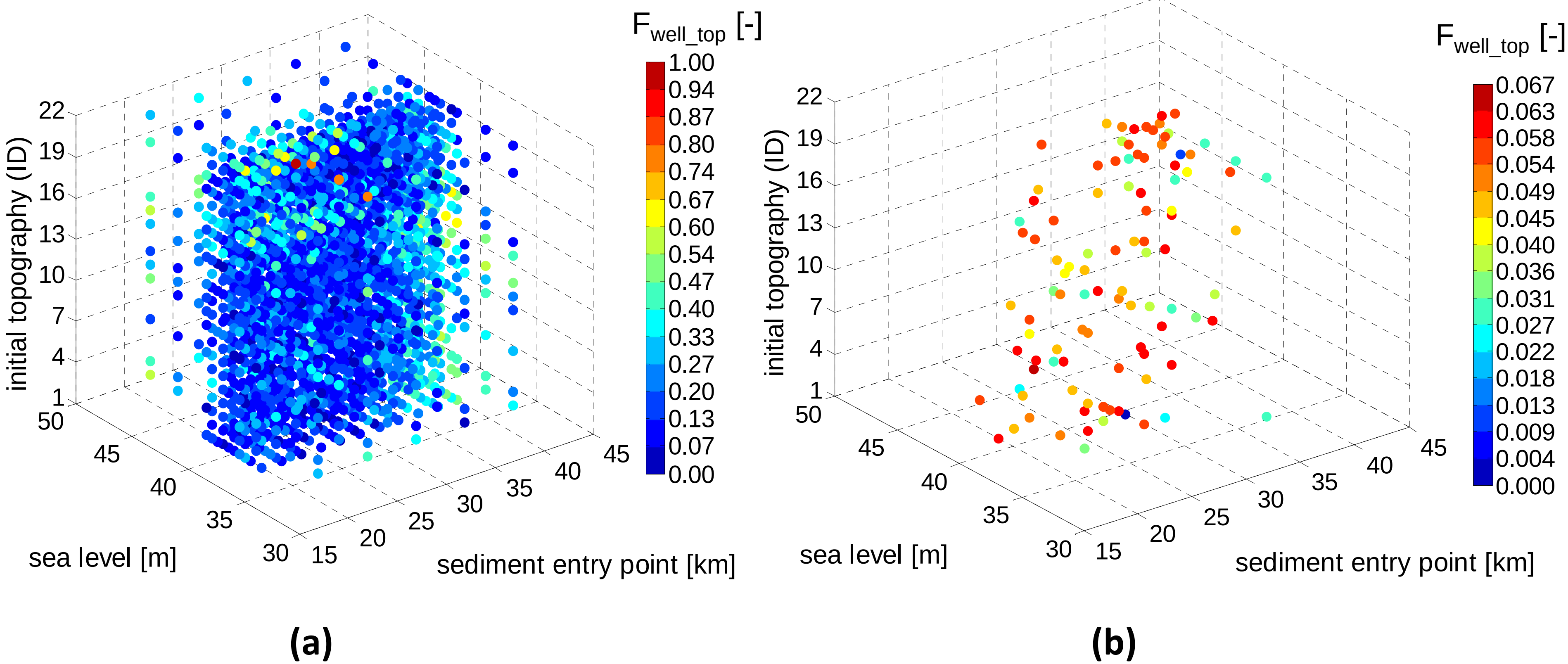

F_well_top [-]
1.00
0.94
0.87
0.80
0.74
0.67
0.60
0.54
0.47
0.40
0.33
0.27
0.20
0.13
0.07
0.00
initial topography (ID)
22
19
16
13
10
7
4
1
50
45
40
35
30
sea level [m]
15
20
25
30
35
40
45
sediment entry point [km]
(a)
F_well_top [-]
0.067
0.063
0.058
0.054
0.049
0.045
0.040
0.036
0.031
0.027
0.022
0.018
0.013
0.009
0.004
0.000
initial topography (ID)
sea level [m]
sediment entry point [km]
(b)

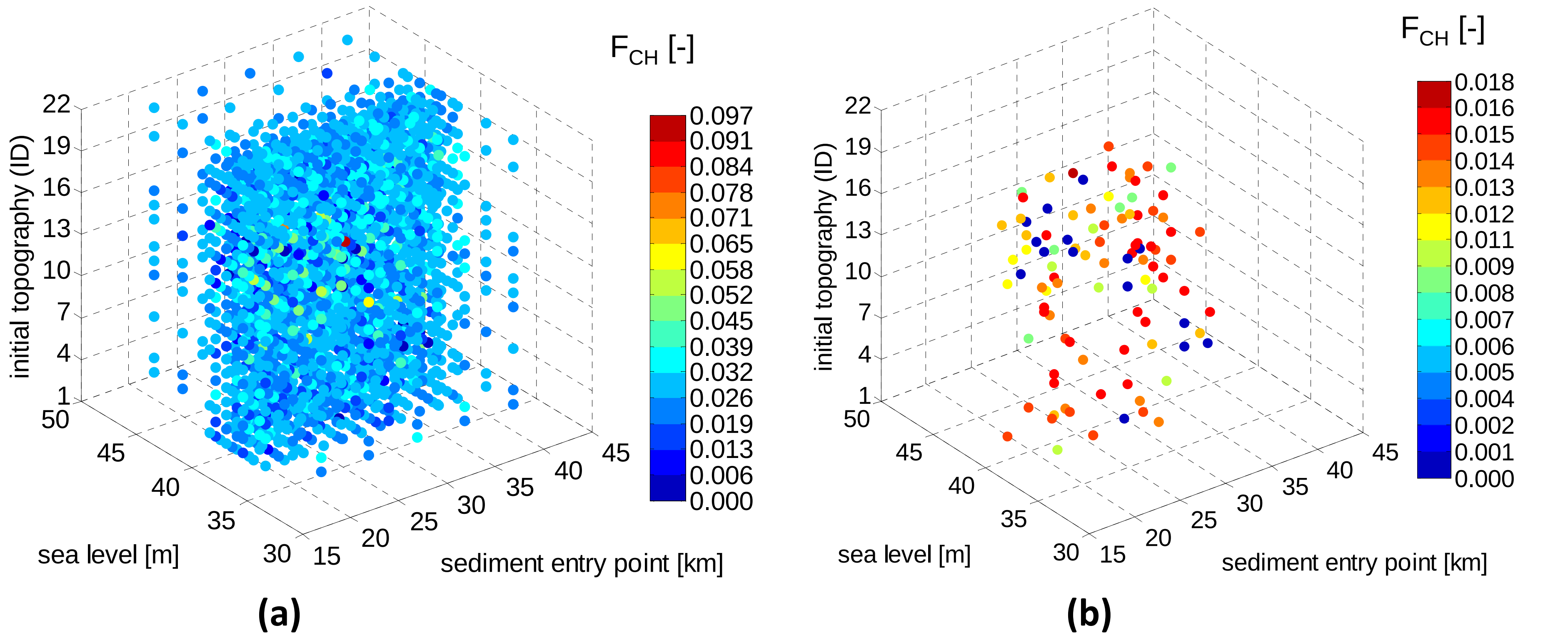

initial topography (ID)
22
19
16
13
10
7
4
1
50
45
40
35
30
sea level [m]
15
20
25
30
35
40
45
sediment entry point [km]
F$_{CH}$ [-]
0.097
0.091
0.084
0.078
0.071
0.065
0.058
0.052
0.045
0.039
0.032
0.026
0.019
0.013
0.006
0.000
(a)
initial topography (ID)
sea level [m]
sediment entry point [km]
F$_{CH}$ [-]
0.018
0.016
0.015
0.014
0.013
0.012
0.011
0.009
0.008
0.007
0.006
0.005
0.004
0.002
0.001
0.000
(b)

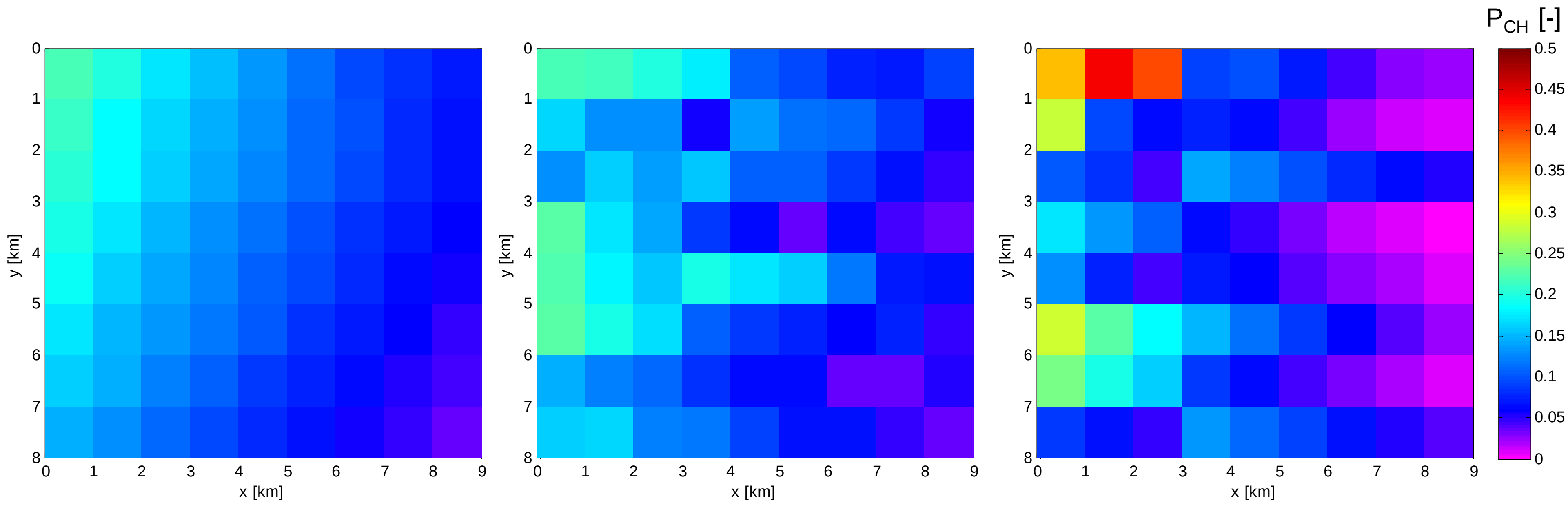

(a)

(b)

(c)

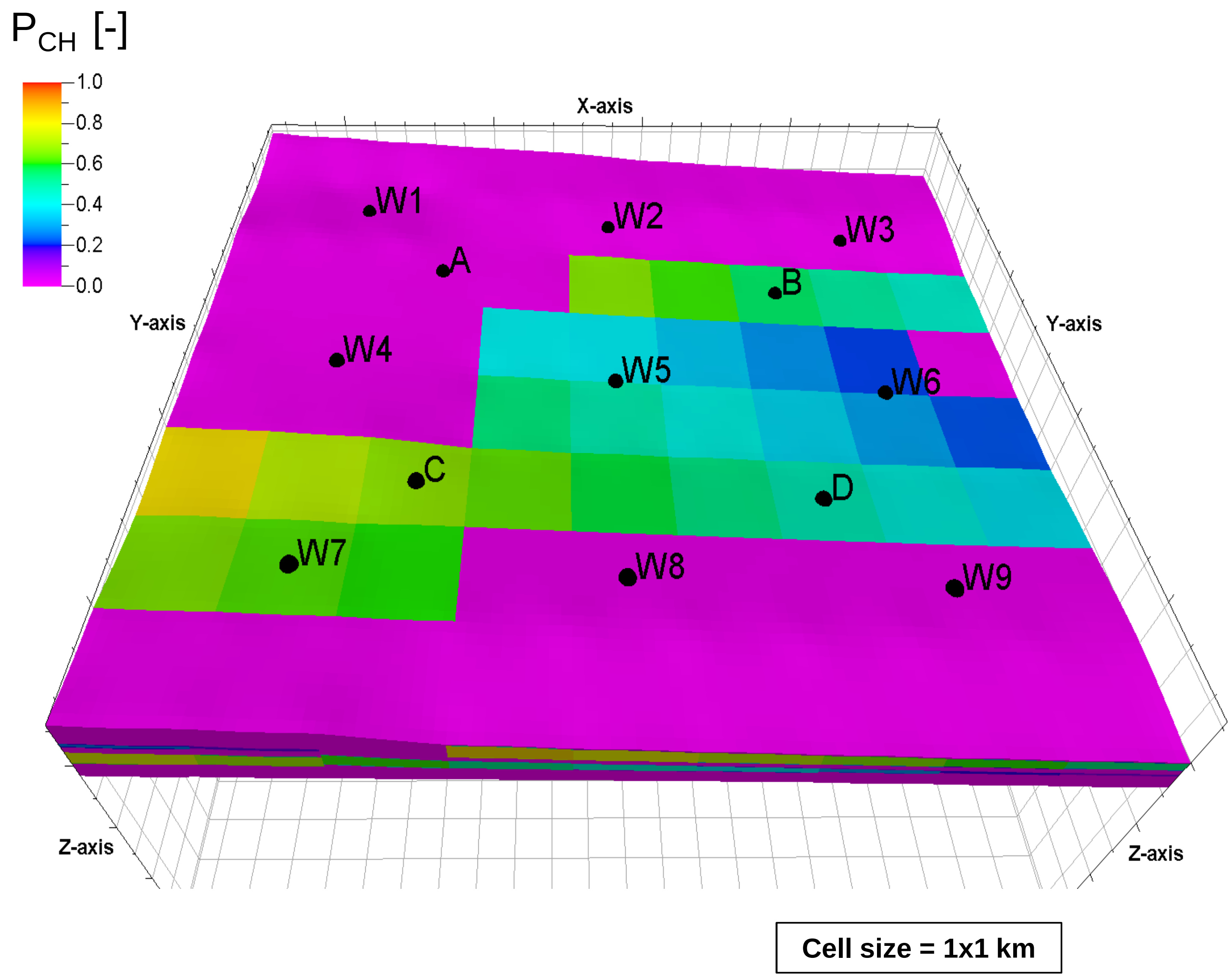

P_CH [-]
1.0
0.8
0.6
0.4
0.2
0.0
X-axis
Y-axis
Y-axis
Z-axis
Z-axis
W1
W2
W3
A
B
W4
W5
W6
C
D
W7
W8
W9
Cell size = 1x1 km

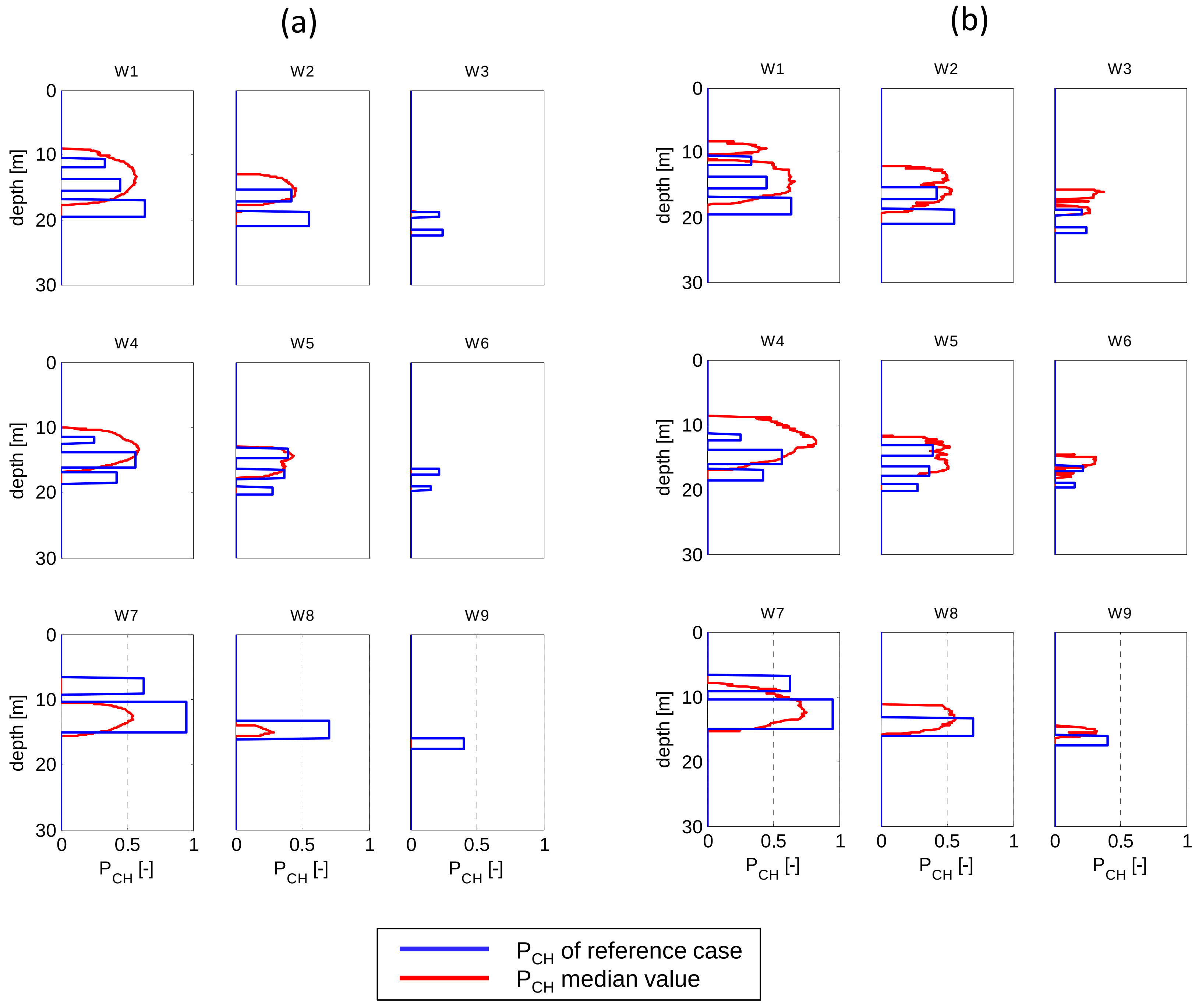

(a)
(b)
W1
W2
W3
W4
W5
W6
W7
W8
W9
depth [m]
P CH [-]
0
10
20
30
0.5
1
P CH of reference case
P CH median value

- Fluvio-deltaic stratigraphy was simulated with a 2DH process-based model
- Goodness of fit functions were used to infer boundary conditions from subsurface data
- Information content of seismic and well data was evaluated
- Depth of reservoir top across basin is best predictor of reservoir lithology